Xanthomonas transcriptome inside cauliflower hydathodes reveals bacterial virulence strategies and physiological adaptation at early infection stages

Running title: *Xanthomonas* transcriptome inside hydathodes

Julien S. Luneau[1,*], Aude Cerutti[1,*], Brice Roux[1,2], Sébastien Carrère[1], Marie-Françoise Jardinaud[1], Antoine Gaillac[1], Carine Gris[1], Emmanuelle Lauber[1], Richard Berthomé[1], Matthieu Arlat[1], Alice Boulanger[1], Laurent D. Noël[1]

Affiliations:

[1] LIPME, université de Toulouse, INRAE, CNRS, université Paul Sabatier, Castanet-Tolosan, France

[2] present address: HalioDx, Luminy Biotech Entreprises, 163 Avenue de Luminy, F-13288 Marseille Cedex 9, France

* These authors contributed equally to this work

Authors for correspondence: alice.boulanger@inrae.fr and laurent.noel@inrae.fr, LIPME, Université de Toulouse, INRAE, CNRS, Université Paul Sabatier, Castanet-Tolosan, France. Tel: +33 5 61 28 50 47.

Abstract

Xanthomonas campestris pv. *campestris* (*Xcc*) bacterium is a seed-transmitted vascular pathogen causing black rot disease on cultivated and wild *Brassicaceae*. *Xcc* enters the plant tissues preferentially via hydathodes which are organs localized at leaf margins. In order to decipher both physiological and virulence strategies deployed by *Xcc* during early stages of infection, the transcriptomic profile of *Xcc* was analyzed three days after entry into cauliflower hydathodes. Despite the absence of visible plant tissue alterations and a bacterial biotrophic lifestyle, 18% of *Xcc* genes undergo a transcriptional reprogramming, including a striking repression of chemotaxis and motility functions. *Xcc* full repertoire of virulence factors was not yet activated but the expression of the 95-gene HrpG regulon, including genes coding for the type three secretion machinery important for suppression of plant immunity, was induced. The expression of genes involved in metabolic adaptations such as catabolism of plant compounds, transport functions, sulfur and phosphate metabolism was upregulated while limited stress responses were observed three days post infection. These transcriptomic observations give information about the nutritional and stress status of bacteria during the early biotrophic infection stages and help to decipher the adaptive strategy of *Xcc* to the hydathode environment.

Word count: 4981

Keywords

Xanthomonas campestris, hydathode, cauliflower, transcriptome, *hrp* gene cluster, type III effector, type III secretion, *hrpG*, adaptation, *in planta*.

Introduction

Xanthomonas campestris pv. *campestris* (*Xcc*) is a seed-transmitted vascular pathogen causing black rot disease on *Brassicaceae.* This bacterium has a complex lifestyle composed of both epiphytic and endophytic stages (1) which have been studied using molecular genetics since the 80's (2). *Xcc* epiphytic life is associated with environmental stresses such as UV or dehydration and relies, for instance, on the production of xanthan exopolysaccharides (EPS) or protective pigments such as xanthomonadin. Upon favorable conditions, *Xcc* will gain access into the leaf inner tissues via wounds or hydathodes (3).

Hydathodes are plant organs localized at the leaf margin mediating guttation. Hydathodes are classically composed of an epidermis with water pores resembling stomata and an inner lose parenchyma called epithem irrigated by numerous xylem vessels (4). These specific structures offer an ecological niche for pathogenic bacteria and a rapid access to xylem vessels leading to systemic vascular infections (3). However, only few pathogens have been demonstrated to colonize this niche and the conditions driving hydathode infection are poorly understood (3, 5-9). While a pre-invasive immunity limiting *Xcc* entry through water pores could not be evidenced, a post-invasive immunity was described inside the epithem (3). This is best revealed by the inability of a bacterial mutant of the Hrp (hypersentive response and pathogenicity) type III secretion (T3S) system to multiply in the epithem and to initiate vascular infections. The T3S system is responsible for the secretion and translocation of type III effector (T3E) proteins inside plant cells where they interfere with plant physiology and suppress plant immunity (10). These results highlight the importance of immune suppression for the establishment of the infection.

Once inside hydathodes, *Xcc* adapts to this niche and adopts a biotrophic lifestyle: bacteria slowly multiply in the apoplastic spaces between epithem cells without causing visible tissue alterations as observed until three days post infection (dpi) of cauliflower hydathodes (3). A

switch to a necrotrophic behaviour is then observed, resulting in the almost complete digestion of the epithem at 6 dpi and *Xcc* vascularization. Systemic infection reaching the flowers will cause seed colonization and transmission to seedlings (11, 12).

During infection, *Xcc* may feed on guttation fluid, xylem sap or plant tissues (13). This process can be facilitated by high affinity nutrient transport systems such as TonB-dependent transporters (TBDT) for mineral (e.g iron) or carbohydrate nutrition (e.g. sucrose, 14) and to a large repertoire of plant cell wall degrading enzymes secreted through the type two secretion (T2S) system. Such metabolic adaptations need to be finely coordinated throughout the infectious cycle. Master regulators include the *rpf*-DSF (Diffusible Signal Factor) quorum sensing system, sensors of nutrient availability and metabolic activity and two-component systems that allow bacterial cells to respond appropriately to diverse extracellular stimuli encountered during its life cycle such as oxidative stress, oxygen levels, pH, temperature and plant signals (15-17). Among them, some are well known to play a major role in virulence such as the response regulator HrpG which is, with the transcription regulator HrpX, the master regulator of the T3S regulon (18-20).

Our knowledge of *Xcc* gene expression *in planta* remains elusive and technically challenging especially at early steps of infection when bacterial populations are low. Indeed, most transcriptomic studies in *Xcc* or other *Xanthomonas* species were performed so far *in vitro* focusing on specific regulons of the *hrpG* and *hrpX* genes in *hrp-inducing* media, of the *prc* protease gene, of the DSF-mediated quorum sensing system or of the *gum* genes responsible for xanthan production (21-31). Only few *in planta* transcriptomic analyses were performed on *Xanthomonas* (28, 32-34) and all at late stages of infection and/or in comparison to *in vitro*-grown bacteria. Such *in planta* transcriptomics approaches would help identify new

pathogenic behaviors and adaptation to the host during the infection process and in the different tissues colonized. Such approaches are also good descriptors of the environmental conditions and stresses imposed by the host to the bacterial pathogen (35).

In this study, we compare the transcriptome of *Xcc* inside cauliflower hydathodes at 4 or 72 hours after inoculation, *i.e.* during the biotrophic stage of infection, in order to determine *Xcc* adaptative transcriptomic responses and to infer the environmental conditions met by this bacterial pathogen inside these plant organs.

Materials and methods

Bacterial strains, plasmids and growth conditions

The list of strains and plasmids used in this study is provided in Table S1. *Xcc* was cultivated in MOKA medium (4 $g.l^{-1}$ Yeast extract, 8 $g.l^{-1}$ Casamino acids, 1 mM $MgSO_4$ and 2 $g.l^{-1}$ K_2HPO_4) at 28°C under agitation at 200 rpm or on MOKA-agar plates (14). *E. coli* strains TG1 and strain carrying pRK2073 helper plasmid were cultivated in liquid LB medium or on LB-agar plates at 37°C under agitation. Antibiotics were used at the following concentrations: 50 µg/ml rifampicin, 50 µg/ml kanamycin, and 40 µg/ml spectinomycin.

Mutagenesis and complementations

In-frame deletion mutants of *Xcc* were obtained by double recombination with derivatives of the suicide plasmid pK18mobSacB as described (36). Sequences flanking the deletion were amplified from *Xcc* strain 8004 genomic DNA and introduced into pK18mobSacB by Gibson assembly (37). For complementation, the CDS was amplified from *Xcc* strain 8004 genomic DNA and cloned by Gibson assembly into plasmid pK18_CompR3, a pK18mobSacB derivative containing a pTac promoter and a T7 terminator region from pCZ1016 (38)

flanked by *XC_1301* and *XC_1302* sequences to drive stable insertion at the *XC_1301*/*XC_1302* interval. For genes lacking ribosome-binding site (RBS) in their upstream region, the RBS from plasmid pK18-GUS-GFP (3) was inserted downstream the pTac promoter giving pK18_compR3_RBS. All plasmids were conjugated into *Xcc* 8004::GUS-GFP derivatives by triparental mating with the *E. coli* TG1 carrying pRK2073 helper plasmid as described (3, 39, 40). The sequences of oligonucleotides used to construct deletion and complementation plasmids are listed in Table S2. The growth of all strains was assessed in MME and MOKA media (Figure S1).

Plant growth conditions

Brassica oleracea var *botrytis* cv. Clovis F1 (cauliflower) were grown under greenhouse conditions. Four-weeks-old plants were transferred one day before inoculations in a growth chamber (9 hours light; 22°C; 70% relative humidity).

Preparation of biological samples used for RNA sequencing

Xcc strains were grown *in vitro* in MOKA medium to mid-exponential phase, harvested by filtration as described (18) and stored at -80°C.

Hydathodes from the first three cauliflower leaves were inoculated by continuous or transient dipping as described (3) using 0.01% of SILWET-L77® (DE SANGOSSE). For continuous dipping, leaves were dipped in a bacterial suspension for 4 hours in a covered small greenhouse and immediately harvested. For transient dipping, leaves were dipped in a bacterial suspension for ca. 15 seconds, watered, placed in a small greenhouse, covered for a day and a half and harvested 72 hours post inoculation. To collect hydathodes, leaves were briefly rinsed twice in sterile distilled water and dried on a paper towel prior to harvesting. At least 1000 hydathodes were macrodissected per condition with a 1.5 mm diameter punch.

Collected tissues were immediately placed in RNA Protect Bacteria Reageant® (Quiagen™, 2:1 (v/v) of RNA Protect and RNAse free water). After three minutes sonication in a water bath, the supernatant was recovered and centrifuged for 10 minutes at 5000g. The pellet was stored at -80°C. Three independent biological replicates were obtained.

To determine the infection level of hydathodes under the two inoculation protocols used, the bacterial populations were determined at 4 and 72 hpi in 24 and 30 individual hydathodes respectively as described below (Figure S2).

RNA extractions, ribodepletion and sequencing

RNA extraction and ribodepletion were performed as previously described (41). Oligonucleotide probes used for RNA depletion were directed against *Xanthomonas* rRNA and 2 tRNA (Ile and Ala) (18) and for plant-derived samples probes targeting Arabidopsis and *Brassica oleracea* rRNA and major chloroplastic RNA (41) (Table S3). RNAs were fractionated into short (<200 nt) and long (>200 nt) RNA fractions using Zymo Research RNA Clean & ConcentratorTM-5 columns (Proteigene) and subjected to oriented sequencing (See supplemental material for detailed procedures). Raw sequence data were submitted to the Sequence Read Archive (SRA) database (Accession SRP280320 and SRP280329).

Reannotation of *Xcc* strain 8004 genome sequence

Annotation of *X. campestris* pv. *campestris* strain 8004 genome was performed using EuGene-PP (41) (EuGene-PP v1.0, eugene-4.1c) with SRP280320 RNA libraries and *X. campestris* pv. *campestris* strains 8004, ATCC33913 and B100 public annotations GCA_000012105.1, GCA_000007145.1 and GCA_000070605.1, respectively. This new annotation is available at https://dx.doi.org/10.25794/reference/id52ofys.

169 **Analysis of RNA sequencing results and statistical analysis**

170 Mapping of RNA sequencing reads was performed on the *Xcc* strain 8004 reannotated
171 genome sequence (42, Genbank accession number CP000050.1) and when appropriate on
172 sequences of *Brassica oleracea* nuclear genome (Brassica_oleracea.v2.1.31; Accession
173 GCA_000695525.1), *Brassica oleracea* mitochondrial genome (accession NC_016118.1) and
174 *Brassica rapa* chloroplastic genome (BRARA_CHL, accession NC_040849.1) as described
175 (18).
176 Differentially expressed genes (DEG) were detected with EdgeR Bioconductor package
177 version 3.30.3 (43). Genes with no counts across all libraries were discarded. Normalization
178 was performed using TMM (trimmed mean of M-values) method (44). Quality control plots
179 of normalized data sets and reproducibility of biological repeats were generated by principal
180 component analysis using Ade4 version1.7-15 package (45) and heatmaps obtained with the
181 package pheatmap version 1.0.12 (Raivo Kolde (2015). pheatmap: Pretty Heatmaps. R
182 package version 1.0.8. https://CRAN.R-project.org/package=pheatmap) on sample-to-sample
183 Euclidean distances.

184 Fitted generalized linear models (GLM) with a design matrix Multiple factor (biological
185 repetition and factor of interest) were designed. The Cox-Reid profile-adjusted likelihood
186 (CR) method in estimating dispersions was used. DEG were called using the GLM likelihood
187 ratio test using a False Discovery Rate (FDR) (46) adjusted q-value < 0.05. Clustering on
188 filtered DEG (q-value < 0.05 in at least on biological condition) was generated with
189 heatmap.2 function as available in the gplots Bioconductor package version 3.0.1. (47) using
190 Ward's minimum variance clustering method on Euclidean (48). Analysis of gene ontology
191 enrichment was conducted using the topGO package version 2.40.0 (49).

192

193 **Infection of hydathodes and measurement of bacterial population**

194 For hydathode infection, the second true leaf of cauliflower plants was dip-inoculated in a
195 bacterial suspension at 10^8 cfu/mL in 1mM $MgCl_2$ containing 0.5% (v/v) Tween 80. In order
196 to determine *Xcc* populations in single hydathodes, hydathodes were collected at three or six
197 days post-inoculation by macrodissection with a 1.5 mm-diameter punch. Eight hydathodes
198 were sampled per leaf and individually placed in 200 µL of 1mM $MgCl_2$. After bead-assisted
199 grinding at 30 Hz for 2 min using a Retsch MM400 grinder, 5-µL droplets of serial dilutions
200 were spotted on MOKA plates supplemented with 30 µg/mL pimaricin in three technical
201 replicates and incubated at 28°C for two to three days. Individual colonies were counted and
202 the mean of the three technical replicates was calculated to estimate the infection level of
203 each hydathode. Experiments were performed on three plants per condition and in three
204 independent biological replicates.
205 Significance of differences observed in bacterial population quantifications and bacterial
206 pathogenicity assays was assessed using the non-parametric Kruskal-Wallis test with α =
207 0.05.
208
209 **Results**
210 **Improved annotation of *Xcc* strain 8004 genome based on a large transcriptomic dataset**
211 Transcriptomic analyses are intrinsically dependent on the proper structural annotation of
212 genes. In order to improve annotation of *Xcc* strain 8004 using experimental expression data,
213 we produced the transcriptome of two nearly isogenic strains grown in MOKA medium:
214 wild-type strain 8004 and strain 8004::*hrpG** which expresses the constitutive active variant
215 E44K of HrpG (50) (see later for comparative analysis of the HrpG regulon). Total RNAs
216 were extracted from exponentially growing bacteria and subjected to ribodepletion as
217 described (18). Small (<200 nt) and large RNA fractions (>200 nt) were subjected to paired-

end and single-end strand-specific sequencing, respectively. RNAs protected by a 5' triphosphate group in the small fraction were used to map precisely transcriptional start sites. Those 13 libraries corresponding to 88 130 260 and 135 564 422 reads from small and large RNA fractions, respectively, were used to refine the annotation of the genome. More than 1724 transcriptional starts (5' UTRs) and 1246 3' UTRs could be experimentally defined (Table 1, https://dx.doi.org/10.25794/reference/id52ofys). Predicted translational start site was modified for 1164 CDS and 753 small ncRNAs were evidenced. These results highlight the importance of experimentally-supported genome annotations and offer improved resources for the functional analysis of *Xcc* transcriptome.

Xcc transcriptome remodeling at early stages of hydathode infection

In order to capture a proxy of the physiological status of *Xcc* at the early step of plant leaf infection, we performed RNA sequencing on bacteria re-isolated from cauliflower hydathodes 72 hours after a rapid dip inoculation of an attached leaf. This 72 hpi timepoint corresponds to a biotrophic phase of the infection where bacteria are still limited to the epitemal apoplastic spaces (3). After four hours of continuous immersion of a detached leaf in the bacterial suspension, ca. 10^5 cfu/hydathode are detected similar to the bacterial titers at 72 hpi (Figure S2). Calculation of Euclidian distances indicated that the 4 hpi transcriptomes cluster with the 72 hpi timepoints rather than *in vitro* samples (Figure S3). This 4 hpi condition was thus chosen as the reference condition since it allows the narrow comparison of two bacterial populations in contact with plant tissues for 4 and 72 hours and a focus on bacterial adaptation to the plant environment.

During hydathode infection (72 hpi versus 4 hpi), *Xcc* massively reshaped its transcriptome with 828 DEGs corresponding to 18% of *Xcc* CDS (Figure 1, Table S4, Table S6). A Gene Ontology (GO) enrichment analysis identified 18 Biological Processes, such as catabolism,

stress response and transport, which were significantly enriched in up-regulated genes (Table 2). On the other hand, 13 GO terms were enriched among downregulated genes, with a strong overrepresentation of motility and chemotaxis categories (Table 2).

Xcc adopts a sedentary lifestyle inside hydathodes

Expression of most genes coding for biosynthesis of flagella and type IV pili and chemotaxis are strongly repressed at 72 hpi. Motility and chemotaxis are key components of pathogenicity, especially for plant pathogens (51). However, *Xcc* seems not to be flagellated when growing in xylem fluids and the motile *Xcc* cells seemed less pathogenic on cauliflower and radish (52). These observations suggest a probable fitness cost of motility during infection. To investigate the importance of motility in disease development, we constructed mutants in key genes for the synthesis of type IV pilus (Δ*pilE* and Δ*pilA*) or flagella (Δ*fliC* and Δ*fliQ*). Single and multiple mutants were tested for *in vitro* motility (Figure S4), pathogenicity (Figure S5) and hydathode colonization (Figure 2). Despite expected *in vitro* motility phenotypes (Figure S4), none of the tested mutant affected disease symptoms development nor hydathode colonization (Figure S5, Figure 2) as it might have been expected for genes whose expression is repressed inside hydathodes. Altogether, these results suggest that motility is a process that is not needed for hydathode infection and maybe costly at this stage of the infection.

Activation of the HrpG regulon at early steps of hydathode infection

hrpG gene is a known master regulator required for the expression of the T3S machinery, T3E proteins and additional genes including plant cell wall degrading enzymes (PCWDE) in *Xanthomonas* spp.. In *Xcc*, expression of *hrpG* and 49 (out of 55) genes coding for the T3S

system and type 3-secreted proteins, was induced at 72 hpi suggesting the involvement of HrpG at this stage of infection (Table S4 and S7). We thus investigated the biological importance of *hrpG* during hydathode infection and studied its regulon.

The 8004Δ*hrpG* mutant showed a 10-fold reduced multiplication in hydathodes at 72 hpi (Figure 2A) and was avirulent on cauliflower after wound inoculation (Figure S5). Both phenotypes could be complemented (Figure 2A and S5). The *hrpG** (E44K) gain-of-function mutation conferring constitutive expression of the HrpG regulon *in vitro* did not affect the multiplication of *Xcc* in cauliflower hydathodes (Figure 2A) nor its pathogenicity after wound inoculation relative to the wild-type strain. As observed in *Xanthomonas euvesicatoria* (20), the 8004::*hrpG** strain also presented a reduced extracellular protease activity (Figure S6B). This suggests that HrpG* *in planta* functions are retained and that *in vitro* studies with this mutant are legitimate.

To determine the extent of the HrpG regulon, we compared the transcriptomes of the 8004::*hrpG** and wild-type strains grown in MOKA medium (Table S4, Table S6). Wild-type strain 8004 does not express *hrp* genes in MOKA in contrast to strain 8004::*hrpG**. Analysis of the HrpG regulon identified 95 DEGs (Log2(fold change) ≥ 2 or ≤ -2, FDR adjusted *p*-value < 0.05) (Table S4). Among the 85 genes with an increased expression in strain 8004::*hrpG**, 43 possess a PIP box promoter motif and are thus likely under *hrpX* control. 39 of the 95 DEGs correspond to genes involved in T3SS and T3Es explaining the enrichment in the GO term "secretion" among genes upregulated in strain 8004::*hrpG** (Table 3, Table S4 and S7). Expression of only 18 out of the 30 genes encoding type 3 secreted proteins was increased in strain 8004::*hrpG** compared to 24 genes at 72 hpi inside hydathodes. Among the other 56 DEGs of the HrpG regulon, 26 encode proteins with unknown function and 19 PCWDE.

The HrpG regulon was almost entirely included in the *in planta* transcriptome (90 out of 95 genes) indicating that HrpG is activated during hydathode infection (Figure 1). Eighteen genes of the HrpG regulon are overexpressed at 4 hpi in comparison to the MOKA condition indicating that expression of the T3S machinery is initiated early during infection (Table S5). Yet, the HrpG regulon (95 genes) remains a very minute part of *Xcc* transcriptomic adaptations to "*in planta"* conditions (828 genes).

Metabolic adaptations of *Xcc* inside hydathodes highlight several nutritional properties of the plant environment

Among the 31 GO terms significantly affected at transcriptomic level, a third are involved in metabolism, indicating that *Xcc* undergoes an important metabolic adaptation inside the hydathode.

- **Modification of the expression profile of genes encoding PCWDE**

We observe an increased transcription of genes involved in the catabolism of cellulose, a major component of primary cell wall. Yet, increased expression of other PCWDE genes is not observed at 72 hpi, consistently with the absence of visible degradation of cell walls in the epithem (3). Among the 43 genes encoding PCWDE in *Xcc* strain 8004 (53), 10 have an increased and 10 a reduced expression at 72 hpi, respectively (Table S7-2). Expression of either *xps* or *xcs* genes encoding type II secretion systems involved in PCWDE secretion is not induced at 72 hpi suggestive of a biotrophic lifestyle.

Lignin is another major component of plant cell walls and a source of aromatic compounds. Interestingly, the expression of *XC_3426* and X*C_3427* genes coding for protocatechuate (PCA) 4;5-dioxygenase subunits is increased 6 and 8 fold at 72 hpi, respectively. PCA is a lignin degradation product (54) which can be further catabolized by PCA dioxygenases to

316 enter the tricarboxylic acid (TCA) cycle (55). While *XC_3426* and *XC_3427* relevance for
317 pathogenicity remains unknown, *XC_0375* to *XC_0383* genes cluster encoding 3- and 4-
318 hydroxybenzoate degrading enzymes are needed for full virulence of *Xcc* in radish (55)
319 suggesting that degradation of plant phenolic compounds happens inside plant tissues.
320
321 • **Expression of transporter genes is deeply remodeled *in planta***
322 Broad expression changes can be observed in transporter genes since 49 out of 210 genes
323 involved in transport are differentially expressed at 72 hpi (Table 2, Table S7-1). Those
324 transporters belong to MFS, ABC and TBDT families. TBDTs have been shown to be
325 involved in iron and carbohydrates polymers uptake with high affinity in *Xcc* (14, 38, 56). 14
326 out of 48 TBDT genes are differentially expressed: 7 show an increased expression at 72 hpi
327 and 7 with a decreased activity. While most have no known function, those which expression
328 is induced by polygalacturonate (PGA) are less expressed at 72 hpi (Table S7-1) (14). The
329 two TBDT genes *XC_3205* and *XC_2512* known to be positively regulated by HrpG and
330 HrpX (14) are induced at 72 hpi.
331 Interestingly, the absence of the *fur* regulon and its iron high affinity TBDT transporters
332 (*XC_0167, XC_3463, XC_2846, XC_1341, XC_1108 XC_0924-0925, XC_0642, XC_4249,*
333 *XC_0558* and *XC_4249*) in our dataset indicates that iron might not be limiting at this stage
334 of hydathode infection.
335
336 • **Upregulation of two pathways important for sulfur assimilation in hydathodes**
337 In contrast to iron, induction of genes important for sulfur transport and assimilation is
338 observed at 72 hpi in hydathodes: the operon encoding the ABC sulfate transporter
339 CysPUWA (*XC_3292* to *XC_3295*) and the operon encoding an assimilatory sulfate
340 reduction pathway leading to sulfide production (*XC_0990* to *XC_0994*) are induced by 6 and

20 fold, respectively (Table S4). Sulfide is then available for cysteine and methionine biosynthesis. Sulfur metabolism including sulfur-containing amino acids, sulfur compounds, or sulfate have been shown to be involved in different virulence factor production, as in xanthan production (57) or T3SS induction (58). Yet, a deletion of the entire *cysPUWA* operon (Δ*XC_3292-95*) in *Xcc* strain 8004 did not significantly affect bacterial multiplication neither in hydathodes after dip-inoculation nor disease symptom development after wound inoculation in cauliflower (Figure 2, Figure S5). Thus, sulfate import through the CysPUWA system is not limiting for bacterial growth in hydathodes or sulfur might be acquired through other import pathways such as the taurine import system. *E. coli* responds to sulfate or cysteine starvation by expressing the *ssuABCDE* and *tauABCD* operons which are involved in the uptake of alkanesulfonate and desulfonation of the organosulfonates and for uptake and desulfonation of taurine, respectively (59, 60). While *ssuABCDE* is absent in *Xcc* strain 8004, TauABCD homologues are encoded by genes of the locus *XC_3454* to *XC_3460* (Figure S7). Interestingly, expression of these genes is increased at 72 hpi suggesting a possible implication of this pathway in sulfur assimilation *in planta*.

- **Phosphate uptake machinery is rate limiting for *Xcc* multiplication inside hydathodes**

Increased expression of the genes encoding the PstSCAB high-affinity transporter system (genes *XC_2708* to *XC_2711*, Table S4) involved in active inorganic phosphate (Pi) import upon phosphate starvation suggests that Pi might be limiting inside hydathodes. This system is known to be activated in various conditions in bacteria (61), including during plant colonization, and is essential for *Xanthomonas axonopodis* pv. *citri* (*Xac*) pathogenicity on citrus (62, 63). In order to test if phosphate acquisition is important for *Xcc* strain 8004 during hydathode colonization, we mutated *XC_2711* (*pstB*) and *XC_3272* which encodes an

366 homologue of the PhoB response regulator important for *E. coli* Pi starvation response (64,
367 65). Results obtained demonstrated that *pstB*, unlike *phoB*, is important for hydathode
368 colonization (Figure 2B) and that both Δ*pstB* and Δ*phoB* mutants caused symptoms similar to
369 the wilt-type strain after direct inoculation into xylem vessels (Figure S5B). These results
370 demonstrate that Pi might be limiting specifically for the growth in hydathodes. Similar to Pi,
371 expression of genes important for nitrogen assimilation such as those involved in uptake of
372 nitrite and nitrate and their reduction to ammonia (*XC_2175* to *XC_2178*) are induced at
373 72 hpi, further stressing the importance of *Xcc* mineral nutritional needs in hydathodes.
374
375 **_Xcc_ adapts to nutritional, osmotic and environmental stresses in hydathodes**
376 Surprisingly, there are limited transcriptional changes for genes associated with transcription,
377 translation, replication, TCA cycle or amino acid biosynthesis between 4 and 72 hpi.
378 However, these functions are already strongly repressed at 4 hpi compared to MOKA
379 conditions indicating that adaptation to the plant environment is associated with a rapid
380 repression of cellular division and core-metabolism. Other stress-responsive genes have an
381 increased expression *in planta* such as base excision and nucleotide excision repair systems,
382 trehalose production pathways, superoxide dismutases and chaperone proteins. In addition,
383 expression of the ABC transporter system *OpuB-ABC* (66, XC_0173 to XC_0174) and the
384 choline degradation pathway (67, XC_0760 to XC_0761), both involved in osmoprotection,
385 are induced 72 hpi suggesting that bacteria face an osmotic shock in the apoplast of the
386 epithem cells (Figure 3, Table S4). Finally, expression of some genes of the *gum* operon
387 (*XC_1658* to *XC_1673*) implicated in the production of the xanthan exopolysaccharides
388 (EPS) are induced by 4- to 5-fold at 72 hpi. Xanthan is a well-known protectant against
389 environmental stresses and toxic compounds and a suppressor of plant immunity (68).

390 Altogether, these data seem to indicate that *Xcc* cells must cope with some nutritional,
391 osmotic and environmental stresses in hydathodes.
392
393 **Discussion**
394 *Xcc* life cycle depends on its adaptation to various plant environments (e.g. seeds, leaf
395 surface, hydathodes, xylem, mesophyll, debris). This work describes the transcriptional
396 changes that *Xcc* undergoes upon plant infection and hydathode colonization, including the
397 regulation of various metabolic and virulence pathways (Figure 3) and informs about the
398 environmental conditions faced by *Xcc* inside hydathodes.
399
400 ***Xcc* adopts a sedentary biotrophic lifestyle inside hydathodes**
401 *Xcc* is a known necrotroph causing black rot disease. However, the physiological snapshot
402 obtained by RNAseq at 72 hpi in hydathodes suggests that *Xcc* behaves as a biotroph since
403 the epithem is intact (69) and many genes coding for degradative enzymes, T2SS and most
404 catabolic pathways of sugar polymers and carbohydrates were expressed at low levels. We
405 also observed that the constitutive activation of the HrpG regulon recapitulating part of the *in*
406 *planta* condition at 72 hpi is associated with a reduced extracellular protease activity. *Xcc*
407 carbon and nitrogen needs could be supported *in planta* by the continuous flow of xylem sap
408 in the epithem. Furthermore, the expression of multiple virulence-associated genes such as
409 those involved in quorum sensing, iron uptake or motility was also reduced at 72 hpi in
410 hydathodes. Though motility has been shown to be an essential virulence trait for many
411 bacterial pathogens (70), *Xcc* motility mutants were not affected in pathogenicity as expected
412 from genes whose expression is repressed in hydathodes. Repression of chemotaxis and
413 motility has also been reported at early rice infection stages in *Xanthomonas oryzae pv.*
414 *oryzicola* (*Xoc*) (34) while twitching motility and quorum sensing were both activated at later

415 infection stages and important for virulence of *Xanthomonas oryzae pv. oryzae* (*Xoo*) (32)
416 and *Xac* (28). Interestingly, an increase in the expression of genes important for twitching
417 motility and adhesion was observed in *Xcc* grown *in vitro* in xylem sap (13). Xylem sap
418 corresponds to the environment met by *Xcc* immediately after leaving the hydathode. These
419 observations suggest a possible biphasic infectious process with the reactivation of the
420 motility and other virulence-associated genes at later infection stages. Further transcriptomic
421 analyses of virulence gene expression throughout the entire infectious cycles would be
422 needed to support such a hemibiotrophic lifecycle of *Xcc*.
423
424 **Stealthiness of *Xcc* inside hydathodes and neutralization of plant immune responses**
425 The observed repression of chemotaxis, twitching and swimming motility also suggests that
426 those functions are dispensable if not detrimental once inside hydathodes. For instance,
427 production of bacterial peptide flg22 from the flagellar FliC protein is a well-known PAMP
428 (pathogen-associated molecular pattern) recognized by the FLS2 receptor and a potent
429 elicitor of basal plant immunity (71). While $flg22_{8004}$ peptide is not recognized by
430 Arabidopsis FLS2 (72, 73), we cannot exclude that other FliC peptides, flagellar proteins or
431 pili proteins from *Xcc* strain 8004 could act as PAMPs in Brassicaceae. In the absence of an
432 *Xcc* strain constitutively expressing those genes, we were not able to test such hypotheses.
433 *Xcc* stealthiness could also be acquired by limiting bacterial multiplication until an efficient
434 suppression of immunity has been achieved. In contrast to a wild-type *Xcc* strain, a T3S
435 system mutant unable to deliver T3E proteins inside plant cells caused hydathode browning
436 and necrosis at 48 hpi and had a reduced multiplication at 72 hpi (3). These results indicate
437 that hydathode immune responses can be effective against bacterial pathogens and that their
438 suppression by *Xcc* T3S system and its T3E proteins is required for successful infection.
439

Inference of environmental conditions inside hydathodes based on *Xcc* transcriptomic behaviour

Compared to *in vitro*-grown *Xcc*, transcriptomic changes are already observed as early as 4 hpi with the increased expression of 14 genes belonging to HrpG regulon (Table S4, Table S5). These genes could participate in the transition from *in vitro* to *in planta* growth such as gene XC_2566 coding for an extracellular function (ECF) sigma factor which importance for this transcriptional switch could be tested. Those transcriptomic profiles can also be used to infer the metabolic and physiological status of *Xcc* inside hydathodes and the nutritional properties of the epithem. For instance, the epithem environment is likely not limiting for assimilable iron since the corresponding uptake machinery is not expressed. In contrast, both the low-affinity phosphate inorganic transport (Pit) and the high-affinity phosphate-specific transport (Pst) systems important for the uptake of inorganic phosphate (Pi) in *Xanthomonas* are upregulated at 72 hpi: (62, 74). Similar to *Xac* (62), *Xcc* Pst system is needed for growth *in planta*. These results demonstrate that *Xcc* not only faces Pi starvation inside hydathodes but that Pi availability also limits *Xcc* proliferation in this tissue. Very low Pi concentrations are indeed found in guttation fluids of several plant species such as barley (75) and are correlated with expression of genes coding for plant high-affinity Pi transporters such as *AtPHT1;4* in hydathodes even under Pi-sufficient conditions (76). These observations suggest that an active competition between the plant and *Xcc* for access to Pi occurs in the epithem. Similar to Pi, *Xcc* transcriptome at 72 hpi also suggests that sulfur and nitrogen are present in low amounts requiring the upregulation of dedicated uptake systems. Yet, it remains unclear whether these elements are limiting for growth of *Xcc* inside hydathodes. Exposure to stresses is also unveiled by the transcriptomic upregulation of genes involved in responses to general stress (e.g. *gum* genes) and osmotic stress. However, it remains uncertain whether osmotic stress is intrinsic of the epithemal environment or whether it is caused by plant immunity. For

instance, we could not evidence significant signs of oxidative stresses classically associated with strong plant immune responses. Therefore, *Xcc* seems to adapt rapidly to the low concentrations of nutrients found in the epithem and to endure limited stress maybe due to the continuous flow of fluids inside hydathodes which renews nutrient supplies and dilutes potential antibacterial compounds.

Such global transcriptomic study provides an averaged picture of the bacterial population *in planta* and will feed functional genomic approaches of *Xcc* pathogenicity.

Acknowledgments

AC and JL were funded by a PhD grant from the French Ministry of Higher Education, Research and Innovation. BR, AC and LDN were funded by grants from the Agence Nationale de la Recherche XANTHOMIX (ANR-2010-GENM-013-02), Xopaque (ANR-10-JCJC-1703-01) and NEPHRON (ANR-18-CE20-0020-01). We are grateful to Stéphanie Bolot for management and early analysis of the Xanthomix dataset. JL, EL, AB and LDN were funded by the XBOX (ANR-19-CE20-JCJC-0014-01) project. The Laboratoire des Interactions Plantes-Microorganismes is part of the French Laboratory of Excellence project (TULIP ANR-10-LABX-41; ANR-11-IDEX-0002-02). All authors benefited from the COST action CA16107 EuroXanth.

Conflict of interest

The authors declare no conflict of interest.

References

1. Vicente JG, Holub EB. *Xanthomonas campestris* pv. *campestris* (cause of black rot of crucifers) in the genomic era is still a worldwide threat to brassica crops. Mol Plant Pathol. 2013;14(1):2-18.

2. Daniels MJ, Barber CE, Turner PC, Sawczyc MK, Byrde RJ, Fielding AH. Cloning of genes involved in pathogenicity of *Xanthomonas campestris* pv. *campestris* using the broad host range cosmid pLAFR1. Embo J. 1984;3(13):3323-8.

3. Cerutti A, Jauneau A, Auriac M-C, Lauber E, Martinez Y, Chiarenza S, et al. Immunity at Cauliflower Hydathodes Controls Systemic Infection by *Xanthomonas campestris* pv *campestris*. Plant Physiol. 2017;174(2):700-16.

4. Cerutti A, Jauneau A, Laufs P, Leonhardt N, Schattat MH, Berthomé R, et al. Mangroves in the Leaves: Anatomy, Physiology, and Immunity of Epithemal Hydathodes. Annu Rev Phytopathol. 2019;57:91-116.

5. Carlton WM, Braun EJ, Gleason ML. Ingress of *Clavibacter michiganensis* subsp. *michiganensis* into Tomato Leaves Through Hydathodes. Phytopathology. 1998;88(6):525-9.

6. Fukui R, Fukui H, McElhaney R, Nelson SC, Alvarez AM. Relationship between symptom development and actual sites of infection in leaves of Anthurium inoculated with a bioluminescent strain of *Xanthomonas campestris* pv *dieffenbachiae*. Appl Environ Microbiol. 1996;62(3):1021-8.

7. Hugouvieux V, Barber CE, Daniels MJ. Entry of *Xanthomonas campestris* pv. *campestris* into hydathodes of *Arabidopsis thaliana* leaves: a system for studying early infection events in bacterial pathogenesis. Molecular plant-microbe interactions 1998;11(6):537-43.

8. Nino-Liu DO, Ronald PC, Bogdanove AJ. *Xanthomonas oryzae* pathovars: model pathogens of a model crop. Mol Plant Pathol. 2006;7(5):303-24.

512 9. Robene-Soustrade I, Laurent P, Gagnevin L, Jouen E, Pruvost O. Specific detection of
513 *Xanthomonas axonopodis* pv. *dieffenbachiae* in anthurium (*Anthurium andreanum)* tissues by
514 nested PCR. Appl Environ Microbiol. 2006;72(2):1072-8.
515 10. Buttner D, Bonas U. Regulation and secretion of *Xanthomonas* virulence factors.
516 FEMS Microbiol Rev. 2010;34(2):107-33.
517 11. Dutta B, Gitaitis R, Sanders H, Booth C, Smith S, Langston DB, Jr. Role of blossom
518 colonization in pepper seed infestation by *Xanthomonas euvesicatoria*. Phytopathology.
519 2014;104(3):232-9.
520 12. Darsonval A, Darrasse A, Durand K, Bureau C, Cesbron S, Jacques MA. Adhesion
521 and fitness in the bean phyllosphere and transmission to seed of *Xanthomonas fuscans* subsp.
522 *fuscans*. Mol Plant Microbe Interact. 2009;22(6):747-57.
523 13. Duge de Bernonville T, Noël LD, SanCristobal M, Danoun S, Becker A, Soreau P, et
524 al. Transcriptional reprogramming and phenotypical changes associated with growth of
525 Xanthomonas campestris pv. campestris in cabbage xylem sap. FEMS Microbiol Ecol.
526 2014;89(3):527-41.
527 14. Blanvillain S, Meyer D, Boulanger A, Lautier M, Guynet C, Denance N, et al. Plant
528 carbohydrate scavenging through TonB-dependent receptors: a feature shared by
529 phytopathogenic and aquatic bacteria. PLoS One. 2007;2(2):e224.
530 15. He YW, Zhang LH. Quorum sensing and virulence regulation in *Xanthomonas*
531 *campestris*. FEMS Microbiol Rev. 2008;32(5):842-57.
532 16. Tao F, He YW, Wu DH, Swarup S, Zhang LH. The cyclic nucleotide monophosphate
533 domain of *Xanthomonas campestris* global regulator Clp defines a new class of cyclic di-
534 GMP effectors. J Bacteriol. 2010;192(4):1020-9.
535 17. Qian W, Han ZJ, He C. Two-component signal transduction systems of *Xanthomonas*
536 spp.: a lesson from genomics. Mol Plant Microbe Interact. 2008;21(2):151-61.

537 18. Roux B, Bolot S, Guy E, Denance N, Lautier M, Jardinaud MF, et al. Genomics and
538 transcriptomics of *Xanthomonas campestris* species challenge the concept of core type III
539 effectome. BMC Genomics. 2015;16:975.
540 19. Zhang HY, Wei JW, Qian W, Deng CY. Analysis of HrpG regulons and HrpG-
541 interacting proteins by ChIP-seq and affinity proteomics in *Xanthomonas campestris*. Mol
542 Plant Pathol. 2020;21(3):388-400.
543 20. Noël L, Thieme F, Nennstiel D, Bonas U. cDNA-AFLP analysis unravels a genome-
544 wide *hrpG*-regulon in the plant pathogen *Xanthomonas campestris* pv. *vesicatoria*. Mol
545 Microbiol. 2001;41(6):1271-81.
546 21. Liao CT, Liu YF, Chiang YC, Lo HH, Du SC, Hsu PC, et al. Functional
547 characterization and transcriptome analysis reveal multiple roles for prc in the pathogenicity
548 of the black rot pathogen *Xanthomonas campestris* pv. *campestris*. Res Microbiol.
549 2016;167(4):299-312.
550 22. Noh TH, Song ES, Kim HI, Kang MH, Park YJ. Transcriptome-Based Identification
551 of Differently Expressed Genes from *Xanthomonas oryzae* pv. *oryzae* Strains Exhibiting
552 Different Virulence in Rice Varieties. Int J Mol Sci. 2016;17(2):259.
553 23. An SQ, Allan JH, McCarthy Y, Febrer M, Dow JM, Ryan RP. The PAS domain-
554 containing histidine kinase RpfS is a second sensor for the diffusible signal factor of
555 *Xanthomonas campestris*. Mol Microbiol. 2014;92(3):586-97.
556 24. Jalan N, Kumar D, Andrade MO, Yu F, Jones JB, Graham JH, et al. Comparative
557 genomic and transcriptome analyses of pathotypes of *Xanthomonas citri* subsp. *citri* provide
558 insights into mechanisms of bacterial virulence and host range. BMC Genomics.
559 2013;14:551.

560 25. Liu W, Yu YH, Cao SY, Niu XN, Jiang W, Liu GF, et al. Transcriptome profiling of
561 *Xanthomonas campestris* pv. *campestris* grown in minimal medium MMX and rich medium
562 NYG. Res Microbiol. 2013;164(5):466-79.
563 26. Zhang F, Du Z, Huang L, Vera Cruz C, Zhou Y, Li Z. Comparative transcriptome
564 profiling reveals different expression patterns in *Xanthomonas oryzae* pv. *oryzae* strains with
565 putative virulence-relevant genes. PLoS One. 2013;8(5):e64267.
566 27. Schmidtke C, Findeiss S, Sharma CM, Kuhfuss J, Hoffmann S, Vogel J, et al.
567 Genome-wide transcriptome analysis of the plant pathogen *Xanthomonas* identifies sRNAs
568 with putative virulence functions. Nucleic Acids Res. 2012;40(5):2020-31.
569 28. Li L, Li J, Zhang Y, Wang N. Diffusible signal factor (DSF)-mediated quorum
570 sensing modulates expression of diverse traits in *Xanthomonas citri* and responses of citrus
571 plants to promote disease. BMC Genomics. 2019;20(1):55.
572 29. Alkhateeb RS, Vorholter FJ, Ruckert C, Mentz A, Wibberg D, Hublik G, et al.
573 Genome wide transcription start sites analysis of *Xanthomonas campestris* pv. *campestris*
574 B100 with insights into the gum gene cluster directing the biosynthesis of the
575 exopolysaccharide xanthan. J Biotechnol. 2016;225:18-28.
576 30. Chen X, Sun C, Laborda P, Zhao Y, Palmer I, Fu ZQ, et al. Melatonin Treatment
577 Inhibits the Growth of *Xanthomonas oryzae* pv. *oryzae*. Front Microbiol. 2018;9:2280.
578 31. Kim S, Cho YJ, Song ES, Lee SH, Kim JG, Kang LW. Time-resolved pathogenic
579 gene expression analysis of the plant pathogen *Xanthomonas oryzae* pv. *oryzae*. BMC
580 Genomics. 2016;17:345.
581 32. Lee SE, Gupta R, Jayaramaiah RH, Lee SH, Wang Y, Park SR, et al. Global
582 Transcriptome Profiling of *Xanthomonas oryzae* pv. *oryzae* under in planta Growth and in
583 vitro Culture Conditions. Plant Pathol J. 2017;33(5):458-66.

584 33. Getaz M, Pulawska J, Smits THM, Pothier JF. Host-Pathogen Interactions between
585 *Xanthomonas fragariae* and Its Host Fragaria x ananassa Investigated with a Dual RNA-Seq
586 Analysis. Microorganisms. 2020;8(8).
587 34. Liao ZX, Ni Z, Wei XL, Chen L, Li JY, Yu YH, et al. Dual RNA-seq of
588 *Xanthomonas oryzae* pv. *oryzicola* infecting rice reveals novel insights into bacterial-plant
589 interaction. PLoS One. 2019;14(4):e0215039.
590 35. Nobori T, Velasquez AC, Wu J, Kvitko BH, Kremer JM, Wang Y, et al.
591 Transcriptome landscape of a bacterial pathogen under plant immunity. Proc Natl Acad Sci U
592 S A. 2018;115(13):E3055-E64.
593 36. Schafer A, Tauch A, Jager W, Kalinowski J, Thierbach G, Puhler A. Small
594 mobilizable multi-purpose cloning vectors derived from the *Escherichia coli* plasmids pK18
595 and pK19: selection of defined deletions in the chromosome of *Corynebacterium*
596 *glutamicum*. Gene. 1994;145(1):69-73.
597 37. Gibson DG, Young L, Chuang RY, Venter JC, Hutchison CA, 3rd, Smith HO.
598 Enzymatic assembly of DNA molecules up to several hundred kilobases. Nat Methods.
599 2009;6(5):343-5.
600 38. Dejean G, Blanvillain-Baufume S, Boulanger A, Darrasse A, Duge de Bernonville T,
601 Girard AL, et al. The xylan utilization system of the plant pathogen *Xanthomonas campestris*
602 pv *campestris* controls epiphytic life and reveals common features with oligotrophic bacteria
603 and animal gut symbionts. New Phytol. 2013;198(3):899-915.
604 39. Figurski DH, Helinski DR. Replication of an origin-containing derivative of plasmid
605 RK2 dependent on a plasmid function provided *in trans* ProcNatlAcadSciUSA.
606 1979;76:1648-52.

607 40. Ditta G, Stanfield S, Corbin D, Helinski DR. Broad host range DNA cloning system
608 for Gram-negative bacteria: Construction of a gene bank of *Rhizobium meliloti*
609 ProcNatlAcadSciUSA. 1980;77:7347-51.
610 41. Sallet E, Roux B, Sauviac L, Jardinaud MF, Carrère S, Faraut T, et al. Next-
611 Generation Annotation of Prokaryotic Genomes with EuGene-P: Application to
612 *Sinorhizobium meliloti* 2011. DNA Res. 2013;20(4):339-54.
613 42. Qian W, Jia Y, Ren SX, He YQ, Feng JX, Lu LF, et al. Comparative and functional
614 genomic analyses of the pathogenicity of phytopathogen *Xanthomonas campestris* pv.
615 *campestris*. Genome Res. 2005;15(6):757-67.
616 43. Robinson MD, Smyth GK. Small-sample estimation of negative binomial dispersion,
617 with applications to SAGE data. Biostatistics. 2008;9(2):321-32.
618 44. Robinson MD, Oshlack A. A scaling normalization method for differential expression
619 analysis of RNA-seq data. Genome Biol. 2010;11(3):R25.
620 45. Dray S, Dufour A-B. The Ade4 package: implementing the duality diagram for
621 ecologists. Journal of Statistical Software. 2007;22(4):1-20.
622 46. Benjamini Y, Yekutieli D. The control of the false discovery rate in multiple testing
623 under dependency. Annals of Statistics. 2001;29:1165-88.
624 47. Warnes G, Bolker B, Bonebakker L, Gentleman R, Huber W, Liaw A, et al. gplots:
625 Various R Programming Tools for Plotting Data. R package version 301
626 https://CRAN.Rproject.org/package=gplots 2016.
627 48. Murtagh F, Legendre P. Ward's Hierarchical Agglomerative Clustering Method:
628 Which Algorithms Implement Ward's Criterion? Journal of Classification. 2014;31(3):274-
629 95.

630 49. Alexa A, Rahnenfuhrer J, Lengauer T. Improved scoring of functional groups from
631 gene expression data by decorrelating GO graph structure. Bioinformatics.
632 2006;22(13):1600-7.
633 50. Guy E, Lautier M, Chabannes M, Roux B, Lauber E, Arlat M, et al. *xopAC*-triggered
634 Immunity against *Xanthomonas* Depends on Arabidopsis Receptor-Like Cytoplasmic Kinase
635 Genes *PBL2* and *RIPK*. PLoS One. 2013;8(8):e73469.
636 51. Matilla MA, Krell T. The effect of bacterial chemotaxis on host infection and
637 pathogenicity. FEMS Microbiol Rev. 2018;42(1).
638 52. Kamoun S, Kado CI. Phenotypic Switching Affecting Chemotaxis, Xanthan
639 Production, and Virulence in *Xanthomonas campestris*. Appl Environ Microbiol.
640 1990;56(12):3855-60.
641 53. da Silva AC, Ferro JA, Reinach FC, Farah CS, Furlan LR, Quaggio RB, et al.
642 Comparison of the genomes of two *Xanthomonas* pathogens with differing host specificities.
643 Nature. 2002;417(6887):459-63.
644 54. Brown CK, Vetting MW, Earhart CA, Ohlendorf DH. Biophysical analyses of
645 designed and selected mutants of protocatechuate 3,4-dioxygenase1. Annu Rev Microbiol.
646 2004;58:555-85.
647 55. Wang JY, Zhou L, Chen B, Sun S, Zhang W, Li M, et al. A functional 4-
648 hydroxybenzoate degradation pathway in the phytopathogen *Xanthomonas campestris* is
649 required for full pathogenicity. Sci Rep. 2015;5:18456.
650 56. Boulanger A, Dejean G, Lautier M, Glories M, Zischek C, Arlat M, et al.
651 Identification and regulation of the N-acetylglucosamine utilization pathway of the plant
652 pathogenic bacterium *Xanthomonas campestris* pv. *campestris*. J Bacteriol.
653 2010;192(6):1487-97.

654 57. Garcia-Ochoa F, Santos VE, Casas JA, Gomez E. Xanthan gum: production,
655 recovery, and properties. Biotechnol Adv. 2000;18(7):549-79.
656 58. Schulte R, Bonas U. A *Xanthomonas* Pathogenicity Locus Is Induced by Sucrose and
657 Sulfur-Containing Amino Acids. Plant Cell. 1992;4(1):79-86.
658 59. Eichhorn E, van der Ploeg JR, Leisinger T. Deletion analysis of the *Escherichia coli*
659 taurine and alkanesulfonate transport systems. J Bacteriol. 2000;182(10):2687-95.
660 60. van Der Ploeg JR, Iwanicka-Nowicka R, Bykowski T, Hryniewicz MM, Leisinger T.
661 The *Escherichia coli ssuEADCB* gene cluster is required for the utilization of sulfur from
662 aliphatic sulfonates and is regulated by the transcriptional activator Cbl. J Biol Chem.
663 1999;274(41):29358-65.
664 61. Lamarche MG, Wanner BL, Crepin S, Harel J. The phosphate regulon and bacterial
665 virulence: a regulatory network connecting phosphate homeostasis and pathogenesis. FEMS
666 Microbiol Rev. 2008;32(3):461-73.
667 62. Moreira LM, Facincani AP, Ferreira CB, Ferreira RM, Ferro MI, Gozzo FC, et al.
668 Chemotactic signal transduction and phosphate metabolism as adaptive strategies during
669 citrus canker induction by Xanthomonas citri. Funct Integr Genomics. 2015;15(2):197-210.
670 63. Pegos VR, Nascimento JF, Sobreira TJ, Pauletti BA, Paes-Leme A, Balan A.
671 Phosphate regulated proteins of *Xanthomonas citri* subsp. *citri*: a proteomic approach. J
672 Proteomics. 2014;108:78-88.
673 64. Yang C, Huang TW, Wen SY, Chang CY, Tsai SF, Wu WF, et al. Genome-wide
674 PhoB binding and gene expression profiles reveal the hierarchical gene regulatory network of
675 phosphate starvation in *Escherichia coli*. PLoS One. 2012;7(10):e47314.
676 65. Gardner SG, McCleary WR. Control of the *phoBR* Regulon in *Escherichia coli*.
677 EcoSal Plus. 2019;8(2).

678 66. Hoffmann T, Warmbold B, Smits SHJ, Tschapek B, Ronzheimer S, Bashir A, et al.
679 Arsenobetaine: an ecophysiologically important organoarsenical confers cytoprotection
680 against osmotic stress and growth temperature extremes. Environ Microbiol. 2018;20(1):305-
681 23.
682 67. Wargo MJ. Homeostasis and catabolism of choline and glycine betaine: lessons from
683 *Pseudomonas aeruginosa*. Appl Environ Microbiol. 2013;79(7):2112-20.
684 68. Kakkar A, Nizampatnam NR, Kondreddy A, Pradhan BB, Chatterjee S. *Xanthomonas*
685 *campestris* cell-cell signalling molecule DSF (diffusible signal factor) elicits innate immunity
686 in plants and is suppressed by the exopolysaccharide xanthan. J Exp Bot. 2015;66(21):6697-
687 714.
688 69. Cerutti A, Auriac M-C, Noël LD, Jauneau A. Histochemical Preparations to Depict
689 the Structure of Cauliflower Leaf Hydathodes. Bio-protocol. 2017;7(20):e2452.
690 70. Chaban B, Hughes HV, Beeby M. The flagellum in bacterial pathogens: For motility
691 and a whole lot more. Seminars in cell & developmental biology. 2015;46:91-103.
692 71. Gomez-Gomez L, Boller T. FLS2: an LRR receptor-like kinase involved in the
693 perception of the bacterial elicitor flagellin in Arabidopsis. Mol Cell. 2000;5(6):1003-11.
694 72. Guy E, Genissel A, Hajri A, Chabannes M, David P, Carrère S, et al. Natural Genetic
695 Variation of *Xanthomonas campestris* pv. campestris Pathogenicity on Arabidopsis Revealed
696 by Association and Reverse Genetics. MBio. 2013;4(3):e00538-12.
697 73. Sun W, Dunning FM, Pfund C, Weingarten R, Bent AF. Within-species flagellin
698 polymorphism in *Xanthomonas campestris* pv *campestris* and its impact on elicitation of
699 Arabidopsis *FLAGELLIN SENSING2*-dependent defenses. Plant Cell. 2006;18(3):764-79.
700 74. Willsky GR, Malamy MH. Characterization of two genetically separable inorganic
701 phosphate transport systems in *Escherichia coli*. J Bacteriol. 1980;144(1):356-65.

75. Nagai M, Ohnishi M, Uehara T, Yamagami M, Miura E, Kamakura M, et al. Ion gradients in xylem exudate and guttation fluid related to tissue ion levels along primary leaves of barley. Plant Cell Environ. 2013;36(10):1826-37.

76. Misson J, Thibaud MC, Bechtold N, Raghothama K, Nussaume L. Transcriptional regulation and functional properties of Arabidopsis Pht1;4, a high affinity transporter contributing greatly to phosphate uptake in phosphate deprived plants. Plant Mol Biol. 2004;55(5):727-41.

Tables

Table 1: Impact of transcriptomic data on the *de novo* annotation of *Xcc* strain 8004 genome

Table 2: GO terms of biological processes enriched among *Xcc* genes differentially expressed in hydathodes (72 hpi vs 4 hpi).

Table 3: GO terms of biological processes enriched among *Xcc* genes belonging to the HrpG regulon.

Figure legends

Figure 1. *Xanthomonas campestris* undergoes a massive transcriptomic reprogramming during hydathodes infection.

(A) Genome-wide expression profile of *Xcc* in hydathodes at 72 hpi versus 4 hpi. Each point represents a gene for which the change in expression level is given as the $\log_2$ fold change (Log_2FC) between 72 hpi and 4 hpi into hydathodes. Genes considered significantly differentially expressed (DEGs) are represented in red if induced or in blue if repressed between the two timepoints. Non DEGs are colored in grey. Genes under the control of the HrpG regulator (*ie*. found differentially expressed in the 8004::*hrpG** vs 8004 dataset) and found differentially expressed at 72 hpi vs 4 hpi in hydathodes are colored in dark red (up-

727 regulated) and dark blue (down-regulated). (B) Venn diagram showing the total number of
728 DEGs ($|Log_2FC| \geq 2$; FDR ≤ 0.05) obtained after growth of the *Xcc* 8004 WT strain in
729 MOKA-rich medium as compared to either the 8004::*hrpG** mutant in MOKA, the WT strain
730 after 4 hours into hydathodes or 72 hours into hydathodes.
731
732 **Figure 2. *Xanthomonas* colonization of hydathodes.**
733 Bacterial multiplication of *Xcc* 8004 wild-type strain (WT), deletion mutants and
734 complemented strains in individual hydathodes 3 and 6 days after dip-inoculation of the
735 second true leaf of 4 weeks-old cauliflower plants. The box plot representations are showing
736 the impact of (A) mutations in the T3SS *hrpG* regulator, (B) mutations in phosphate and
737 sulfate transport genes and, (C) mutations in motility genes over *Xcc* multiplication into
738 hydathodes. Each point of the plot represents the population extracted from one hydathode.
739 At least eight </i> hydathodes were sampled on one leaf per plant and three plants were used
740 per experiment, though not all hydathodes were infected. Results from at least three
741 independent experiments were pooled and a total of at least 50 infected hydathodes were
742 counted for each strain. Letters indicate statistically different groups obtained from the
743 Kruskal-Wallis test on all data points for each strain with an error $\alpha = 0.05$.
744
745 **Figure 3. Schematic representation of *Xcc* main transcriptomic responses happening**
746 **during the early step of hydathode infection.** Genes corresponding to blue and red objects
747 are repressed and induced between 4 and 72 hpi, respectively. Genes corresponding to grey
748 objects are not differentially expressed. T3SS: type three secretion system; T3E: type three
749 effector; T2SS: type two secretion system; LPS: lipopolysaccharide; PCWDE: Plant cell wall
750 degrading enzymes; T4P: type four pilus. Figure drafted using biorender
751 (https://app.biorender.com).

Supplemental Tables

Table S1: List of strains and vectors used in this study

Table S2: Sequences of oligonucleotides used for construction of deletion and complementation plasmids

Table S3: Sequences of oligonucleotides used for oligocapture of plant RNAs

Table S4: Differentialy expressed genes in each condition tested.

Table S5: List of genes belonging to HrpG regulon already differentially expressed after 4 hpi into hydathodes.

Table S6: Complete results of the RNAseq experiments.

Table S7: Summary of *in planta* RNAseq results sorted for specific biological functions.

Table S8: Properties of RNAseq libraries from *Xcc* strain 8004 wild-type and derivatives grown *in vitro* or harvested from cauliflower hydathodes.

Supplemental Figures

Figure S1. Growth of *Xcc* wild-type and mutant strains in MME minimal medium (A) and MOKA rich (B) medium.

Figure S2. Measure of hydathode population in the two conditions used for RNAseq.

Figure S3. RNAseq samples clustering.

Figure S4. Swimming motility assessment in type IV pilus and flagellum mutants in *Xcc*.

Figure S5. Evaluation of disease symptoms severity during infection of cauliflower leaves by *Xcc* mutants.

Figure S6. Phenotypic characterization of *hrpG* mutants.

Figure S7. Synteny of genes involved in two transport systems in *Xcc*.

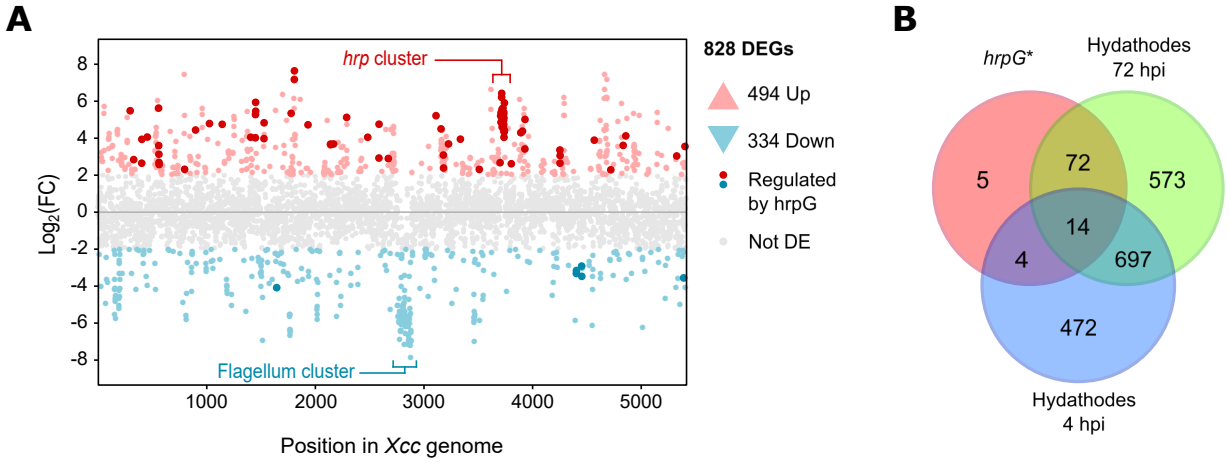

Figure 1. *Xanthomonas campestris* undegoes a massive transcriptomic reprogramming during hydathodes infection.

(A) Genome-wide expression profile of *Xcc* in hydathodes at 72 hpi versus 4 hpi. Each point represents a gene for which the change in expression level is given as the Log_2 Fold Change between 72 hpi and 4 hpi into hydathodes. Genes considered significantly differentially expressed (DE Genes) are represented in red when if induced or in blue if reppressed between the two timepoints. Non-differentially expressed genes are colored in grey. Genes under the control of the HrpG regulator (ie. found differentially expressed in the 8004::*hrpG** vs 8004 dataset) and found differentially expressed at 72 hpi vs 4 hpi in hydathodes are colored in dark red (up-regulated) and dark blue (down-reguated). (B) Venn diagram showing the total number of DEGs ($|Log_2FC| > 2$; FDR < 0.05) obtained after growth of the *Xcc* 8004 WT strain in MOKA rich medium as compared to either the 8004::*hrpG** mutant in MOKA, the WT strain after 4 hours into hydathodes or the WT strain after 72 hours into hydathodes.

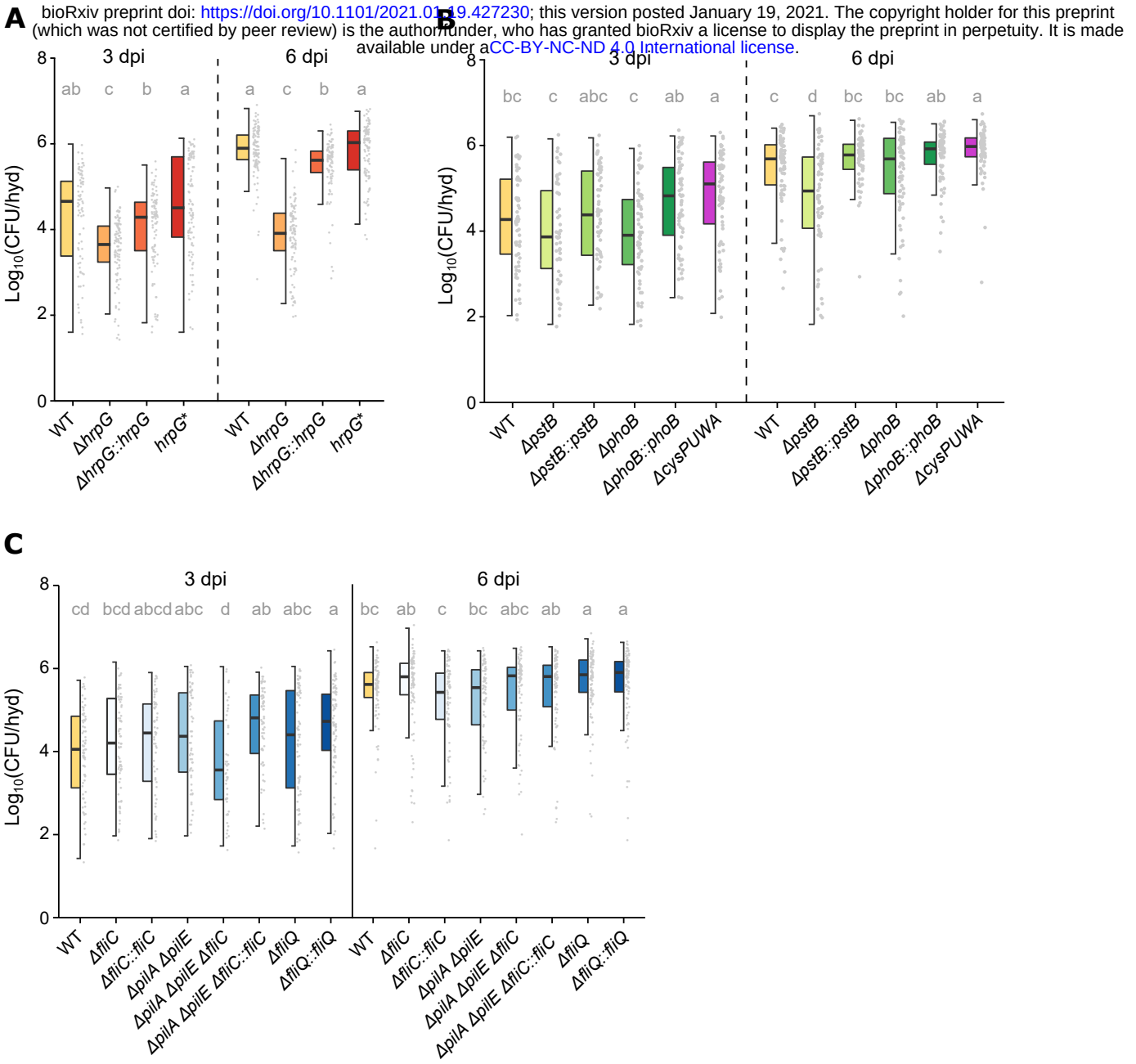

Figure 2. *Xanthomonas* colonization of hydathodes.

Bacterial multiplication of *Xcc* 8004 wild-type strain (WT), deletion mutants and complemented strains in individual hydathodes 3 and 6 days after dip-inoculation of the second true leaf of 4 weeks-old cauliflower plants. The box plot representations are showing the impact of (A) mutations in the T3SS *hrpG* regulator, (B) mutations in phosphate and sulfate transport genes and, (C) mutations in motility genes over *Xcc* multiplication into hydathodes. Each point of the plot represents the population extracted from one hydathode. At least 8 hydathodes were sampled on one leaf per plant and three plants were used per experiment, though not all hydathodes were infected. Results from at least three independent experiments were pooled and a total of at least 50 infected hydathodes were counted for each strain. Letters indicate statistically different groups obtained from the Kruskal-Wallis test on all data points for each strain with an error $\alpha = 0.05$.

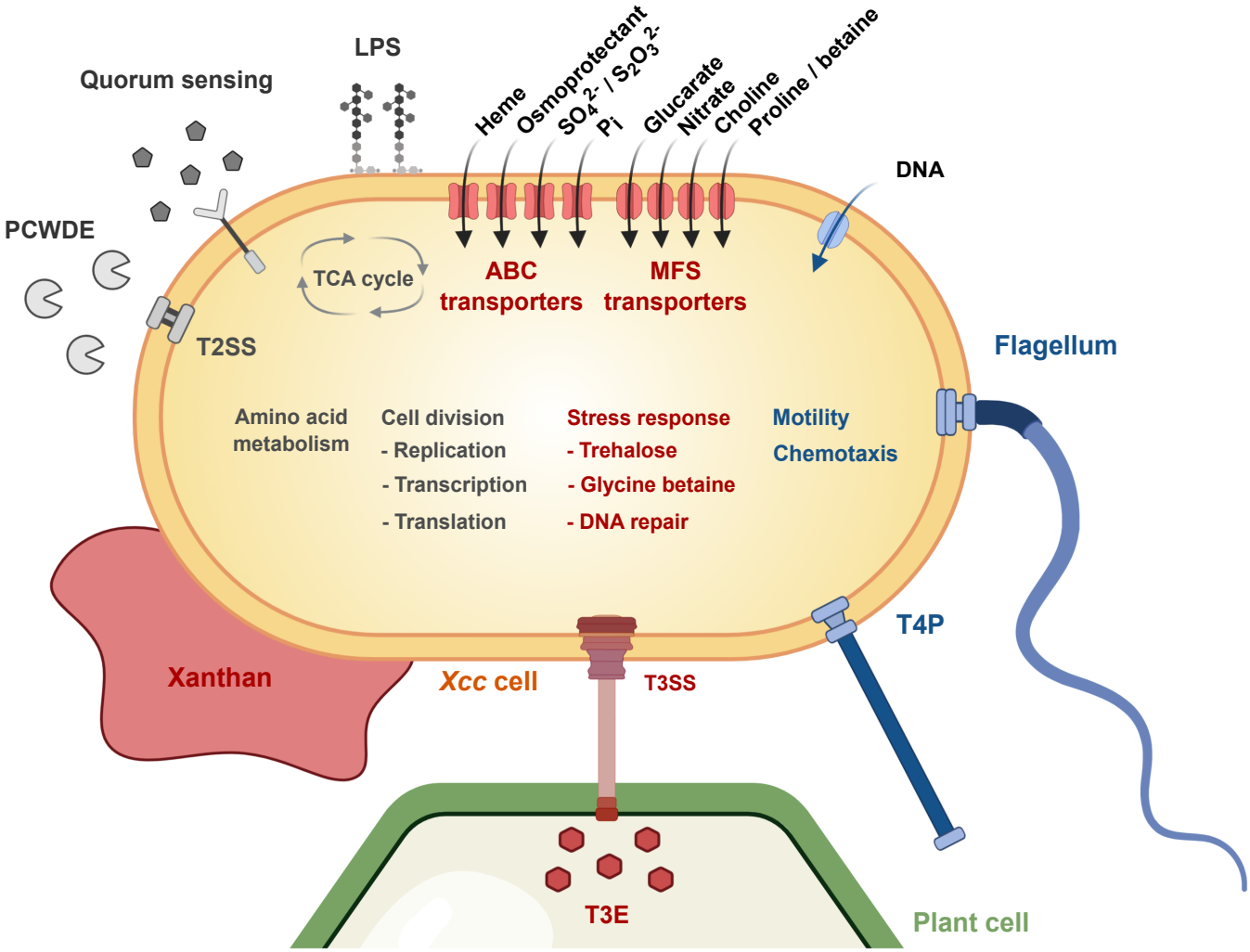

Figure 3. Schematic representation of *Xcc* main transcriptomic responses happening during the early steps of hydathode infection.Genes corresponding to blue and red objects are repressed and induced between 4 and 72 hpi, respectively. Genes corresponding to grey objects are not differentially expressed. T3SS: type three secretion system; T3E: type three effector; T2SS: type two secretion system; LPS: lipopolysaccharide; PCWDE: Plant cell wall degrading enzymes; T4P: type four pilus. Figure drafted using biorender (https://app.biorender.com).

Table 1: Impact of transcriptomic data on the *de novo* annotation of *Xcc* strain 8004 genome

RNAseq data used[a]	All genes	mRNA[b]	rRNA[c] operon	tRNA[d]	Other ncRNA[e]	5' UTR[f]	3' UTR[g]	Reference	Accession Number
No	4333	4273	2	53	1	-	-	Qian et al., 2005	NCBI:CP000050.1
No	4631	4478	2	54	93	-	-	NCBI	NCBI:NC_007086.1
Yes	5431	4617	2	55	753	1724	1246	This study	DOI:10.25794/reference/id52ofys

[a] Use of merged transcriptomic datasets from *Xcc* strain 8004 derivatives (WT or 8004::*hrpG**) grown *in vitro* in MOKA medium.
[b] Protein coding sequence
[c] Ribosomal RNA
[d] Tranfer RNA
[e] Non coding RNA
[f] 5' untranslated region
[g] 3' untranslated region

Table 2: GO terms of biological processes enriched among *Xcc* genes differentially expressed in hydathodes (72 hpi vs 4 hpi).

GO.ID	Term	Annotated[a]	Significant[b]	Expected[c]	Adjust p Value
Upregulated					
GO:0006073	cellular glucan metabolic process	19	11	1,89	$1.8\ 10^{-8}$
GO:0055114	oxidation-reduction process	399	74	39,78	$8.9\ 10^{-8}$
GO:0070814	hydrogen sulfide biosynthetic process	5	5	0,5	$9.5\ 10^{-6}$
GO:0005992[e]	**trehalose biosynthetic process**	**5**	**5**	**0,5**	**$9.5\ 10^{-6}$**
GO:0006950	response to stress	123	25	12,26	0.00063
GO:0019344	cysteine biosynthetic process	6	4	0,6	0.00123
GO:0009251	glucan catabolic process	11	5	1,1	0.00263
GO:0043649	dicarboxylic acid catabolic process	7	4	0,7	0.00265
GO:0044247	cellular polysaccharide catabolic process	8	4	0,8	0.00361
GO:0009306	protein secretion	46	11	4,59	0.00435
GO:0043623	cellular protein complex assembly	18	6	1,79	0.00612
GO:0006457	protein folding	18	6	1,79	0.00612
GO:0098661	inorganic anion transmembrane transport	15	5	1,5	0.01230
GO:0098869	cellular oxidant detoxification	30	7	2,99	0.02468
GO:0044419	interspecies interaction between organisms	12	4	1,2	0.02506
GO:0005975	carbohydrate metabolic process	201	39	20,04	0.03559
GO:0006817	phosphate ion transport	8	3	0,8	0.03753
GO:0016311	dephosphorylation	33	7	3,29	0.04006
Downregulated					
GO:0006935	chemotaxis	44	36	3,12	$< 10^{-30}$
GO:0097588	**archaeal or bacterial-type flagellum-dependent cell motility**	**23**	**23**	**1,63**	**$9.4\ 10^{-28}$**
GO:0007165	signal transduction	175	51	12,4	$1.7\ 10^{-22}$
GO:0044781	**bacterial-type flagellum organization**	**16**	**16**	**1,13**	**$2.2\ 10^{-19}$**
GO:0030031	cell projection assembly	16	13	1,13	$3.5\ 10^{-13}$
GO:0000160	phosphorelay signal transduction system	133	23	9,43	$3.5\ 10^{-5}$
GO:0000272	polysaccharide catabolic process	27	7	1,91	0.0021

GO:0007155	cell adhesion	5	3	0,35	0.0031
GO:0048870	**cell motility**	**25**	**25**	**1,77**	**0.0039**
GO:0071554	cell wall organization or biogenesis	40	6	2,83	0.0149
GO:0006468	protein phosphorylation	79	11	5,6	0.0215
GO:0015031	protein transport	81	12	5,74	0.0295
GO:0000302	response to reactive oxygen species	11	3	0,78	0.0378

[a] Number of genes annotated for a given GO term
[b] Number of differentially regulated genes among the genes annotated for a given GO term
[c] Expected number of differentially regulated genes if no significant enrichment
[e] Terms for which all annotated genes are differentially regulated are highlighted in bold

Table 3: GO terms of biological processes enriched among *Xcc* genes belonging to the HrpG regulon.

GO.ID	Term	Annotated[a]	Significant[b]	Expected[c]	adjusted p Values
BIOLOGICAL PROCESS					
Upregulated					
GO:0002790	peptide secretion	46	9	0,91	$1.5\ 10^{-7}$
GO:0009306	protein secretion	46	9	0,91	$1.5\ 10^{-7}$
GO:0032940	secretion by cell	47	9	0,93	$1.8\ 10^{-7}$
GO:0046903	secretion	47	9	0,93	$1.8\ 10^{-7}$
GO:0015031	protein transport	81	10	1,61	$2.5\ 10^{-6}$
GO:0008104	protein localization	85	10	1,69	$3.9\ 10^{-6}$
GO:0015833	peptide transport	85	10	1,69	$3.9\ 10^{-6}$
GO:0045184	establishment of protein localization	85	10	1,69	$3.9\ 10^{-6}$
GO:0042886	amide transport	86	10	1,71	$4.3\ 10^{-6}$
GO:0033036	macromolecule localization	96	10	1,91	$1.2\ 10^{-5}$
GO:0071705	nitrogen compound transport	120	10	2,38	$8.6\ 10^{-5}$
GO:0071702	organic substance transport	142	10	2,82	0.00035
GO:0044419	interspecies interaction between organisms	12	3	0,24	0.00143
GO:0051704	multi-organism process	21	3	0,42	0.00763
Downregulated					
GO:0000272	polysaccharide catabolic process	27	3	0,08	$5.6\ 10^{-5}$
GO:0009057	macromolecule catabolic process	58	3	0,18	0.00057
GO:0016052	carbohydrate catabolic process	61	3	0,19	0.00066
GO:0005976	polysaccharide metabolic process	64	3	0,2	0.00076
GO:0005975	carbohydrate metabolic process	201	4	0,63	0.00198
MOLECULAR FUNCTION					
Upregulated					
GO:0016301	kinase activity	176	8	2,71	0.0046
GO:0001067	regulatory region nucleic acid binding	27	3	0,42	0.0077
GO:0044212	transcription regulatory region DNA binding	27	3	0,42	0.0077

GO:0016798	hydrolase activity, acting on glycosyl bonds	83	5	1,28	0.0081
Downregulated					
GO:0004175	endopeptidase activity	57	3	0,17	0.00045
GO:0004252	serine-type endopeptidase activity	30	2	0,09	0.00315
GO:0070011	peptidase activity, acting on L-amino acid peptides	128	3	0,38	0.00477
GO:0008233	peptidase activity	152	3	0,45	0.00774
GO:0016829	lyase activity	158	3	0,46	0.00863
GO:0008236	serine-type peptidase activity	53	2	0,16	0.00964
GO:0017171	serine hydrolase activity	53	2	0,16	0.00964

[a] Number of genes annotated for a given GO term
[b] Number of differentially regulated genes among the genes annotated for a given GO term
[c] Expected number of differentially regulated genes if no significant enrichment

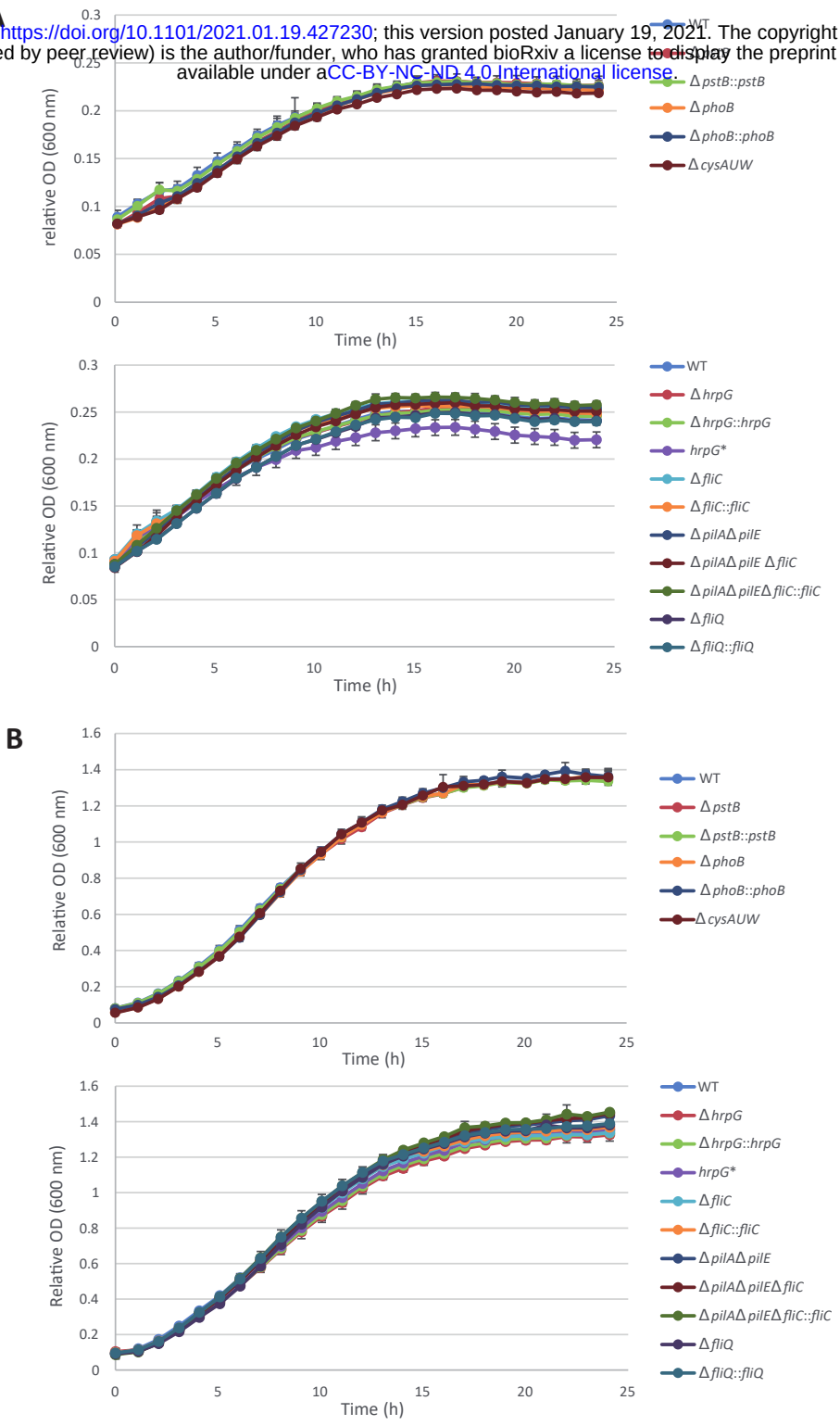

Figure S1: Growth of Xcc wild-type and mutant strains in MME minimal medium (A) and MOKA rich (B) medium.

After overnight growth in complete medium, cells were harvested, washed, and resuspended in MME or MOKA. The error bars indicate the standard deviations obtained from 4 technical replicates. The experiments were repeated 3 times an d similar results were obtained.

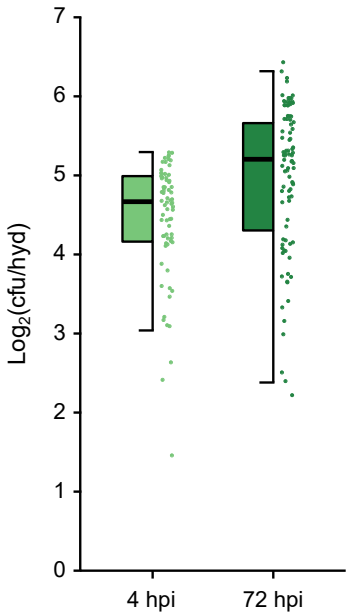

Figure S2. Measure of hydathode population in the two conditions used for RNAseq.
The number of *Xcc* colony forming units (cfu) per hydathode (hyd) was determined after 4 hours of continuous dipping (4 hpi) or 72 hours after transient dipping (72 hpi) for 24 or 30 individual hydathodes respectively in three independent biological replicates. Each point of the plot represents the population extracted from one hydathode. Box plots represent the pooled results obtained from three independent experiments.

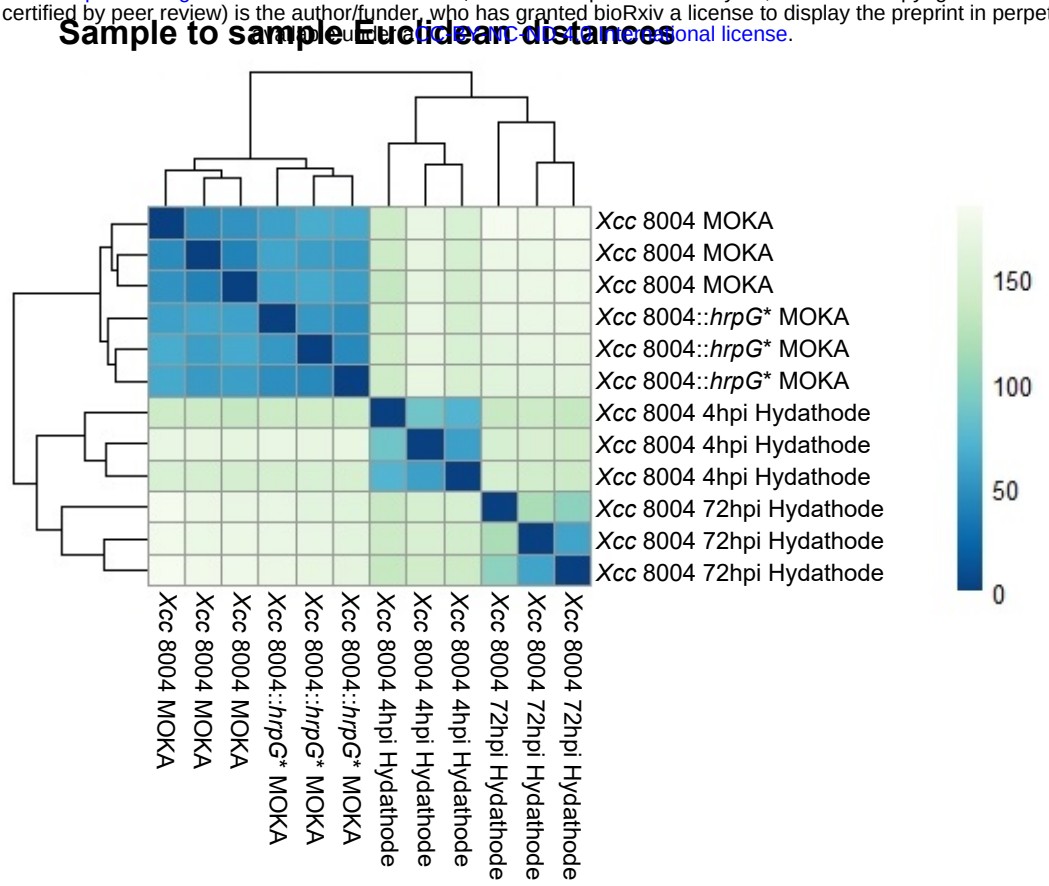

Figure S3. RNAseq samples clustering.

The heatmap shows the Euclidian distances between samples as calculated from the variance-stabilizing data transformation of the count data.

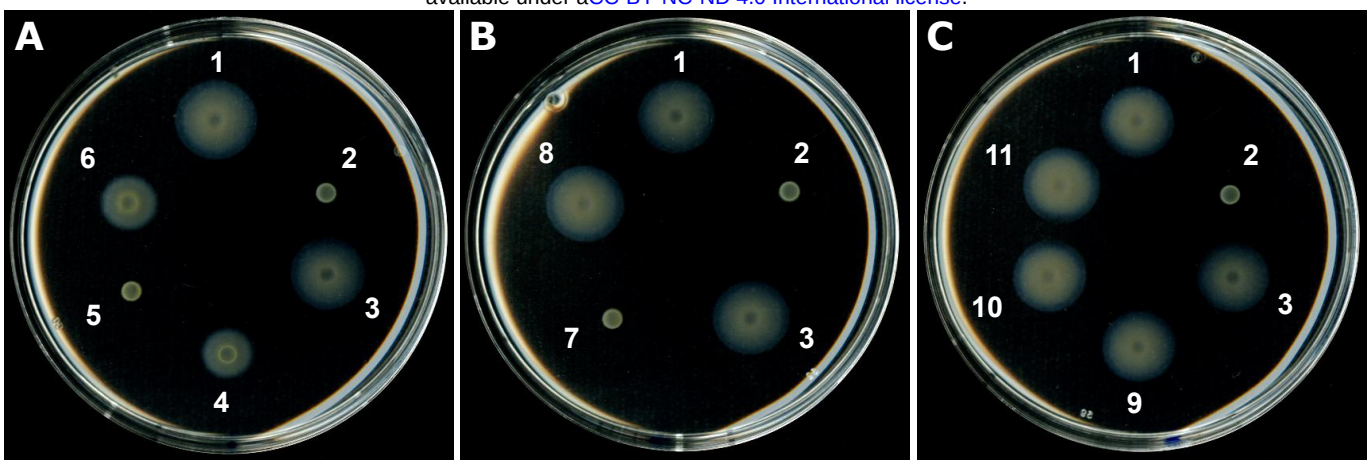

Figure S4. Swimming motility assessment in type IV pilus and flagellum mutants in *Xcc*.
To confirm the loss of flagellar motility in the mutants tested in patho-assays, we assayed their ability to move in 0.3% agar swimming plates. 2 µl of bacterial suspensions adjusted to 10^8 cfu/ml were spotted on swimming plates and pictures were taken after 48 hours of incubation at 28°C. Deletion mutants affected in key components of the type IV pilus (A) and flagellum (B) display reduced and abolished swimming motility respectively. (C) No change in motility was however observed with the Δ*hrpG* and *hrpG** strains.
Strains:
1. WT; 2. Δ*fliC*; 3. Δ*fliC::fliC*; 4. Δ*pilA* Δ*pilE*; 5. Δ*pilA* Δ*pilE* Δ*fliC*; 6. Δ*pilA* Δ*pilE* Δf*liC::fliC*
7. Δ*fliQ*; 8. Δf*liQ::fliQ*; 9. Δ*hrpG*; 10. Δ*hrpG::hrpG*; 11. *hrpG**

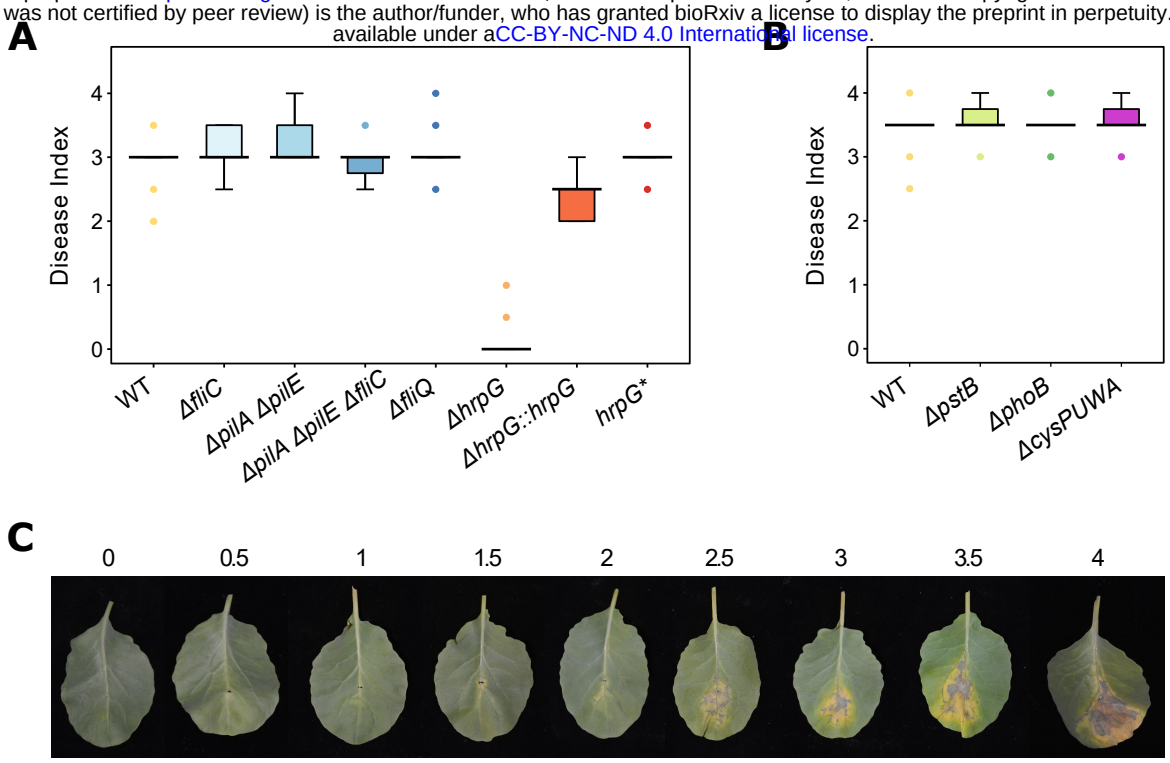

Figure S4. Evaluation of disease symptoms severity during infection of cauliflower leaves by *Xcc* mutants. Severity of the symptoms observed on cauliflower leaves 10 days after inoculation by the *Xcc* 8004::GUS-GFP WT strain or various genetic mutants in (A) motility and T3S regulation or (B) phosphate and sulfate metabolism. The inoculation is performed by piercing the main vein of the second leaf of 4-weeks old cauliflower plants with a needle dipped in a bacterial suspension adjusted to 10^8 cfu/mL. Boxplots represent the results obtained in three independent biological replicates comprising 5 plants per strain each. (C) Disease Index scale designed in this study to score the severity of the symptoms caused by *Xcc* after inoculation into the main vein of the cauliflower leaf. 0 : No symptoms; 0.5 : Mesophyll discoloration; 1 : Mesophyll discoloration & necrosis along the veins; 1.5 : Vein necrosis & yellow chlorosis at the inoculation point; 2 : Vein necrosis & yellow chlorosis extended to the mesophyll; 2.5 : Extended chlorosis & multiple necrosis spots in the mesophyll away from the inoculation point; 3 : Large chlorosis covering all the diseased area; 3.5 : Large necrosis & large chlorosis area reaching the leaf margin; 4 : Necrosis covering all the diseased area.

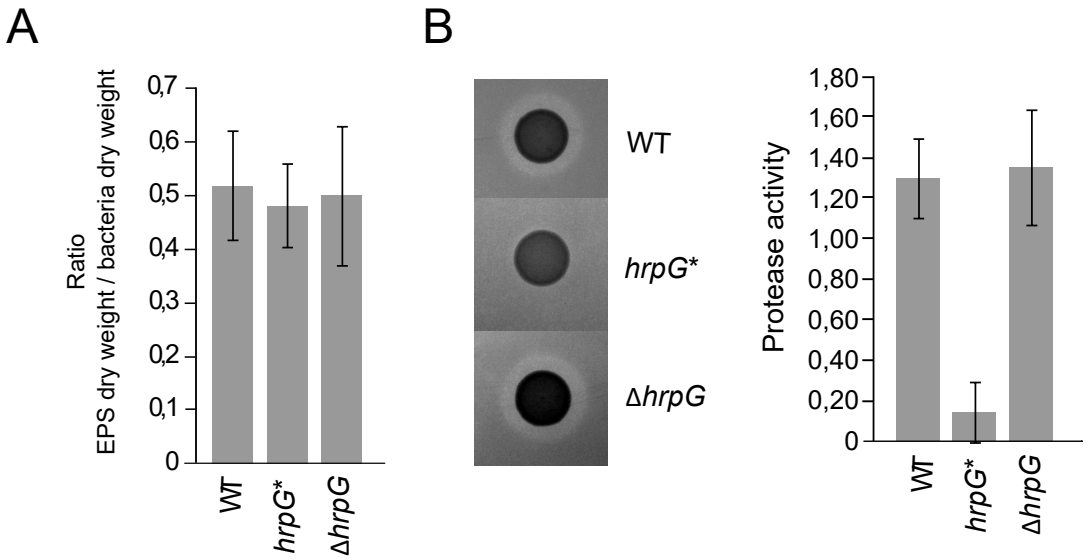

Figure S6. Phenotypic characterization of *hrpG* mutants.

(A) EPS production assays were performed on 24 h growth of either 8004::*GUS-GFP* strain (WT), *hrpG** and Δ*hrpG* strains in rich MOKA medium. Production was normalized on dry weight bacteria. Histogram represents the average of results obtained for three independent replicates. (B) On the left, representative pictures of protease activity assay on plate are shown for each tested strain. The histogram represents the average of protease activity measured, as described in the Supplemental Material and Methods section, for three independent replicates.

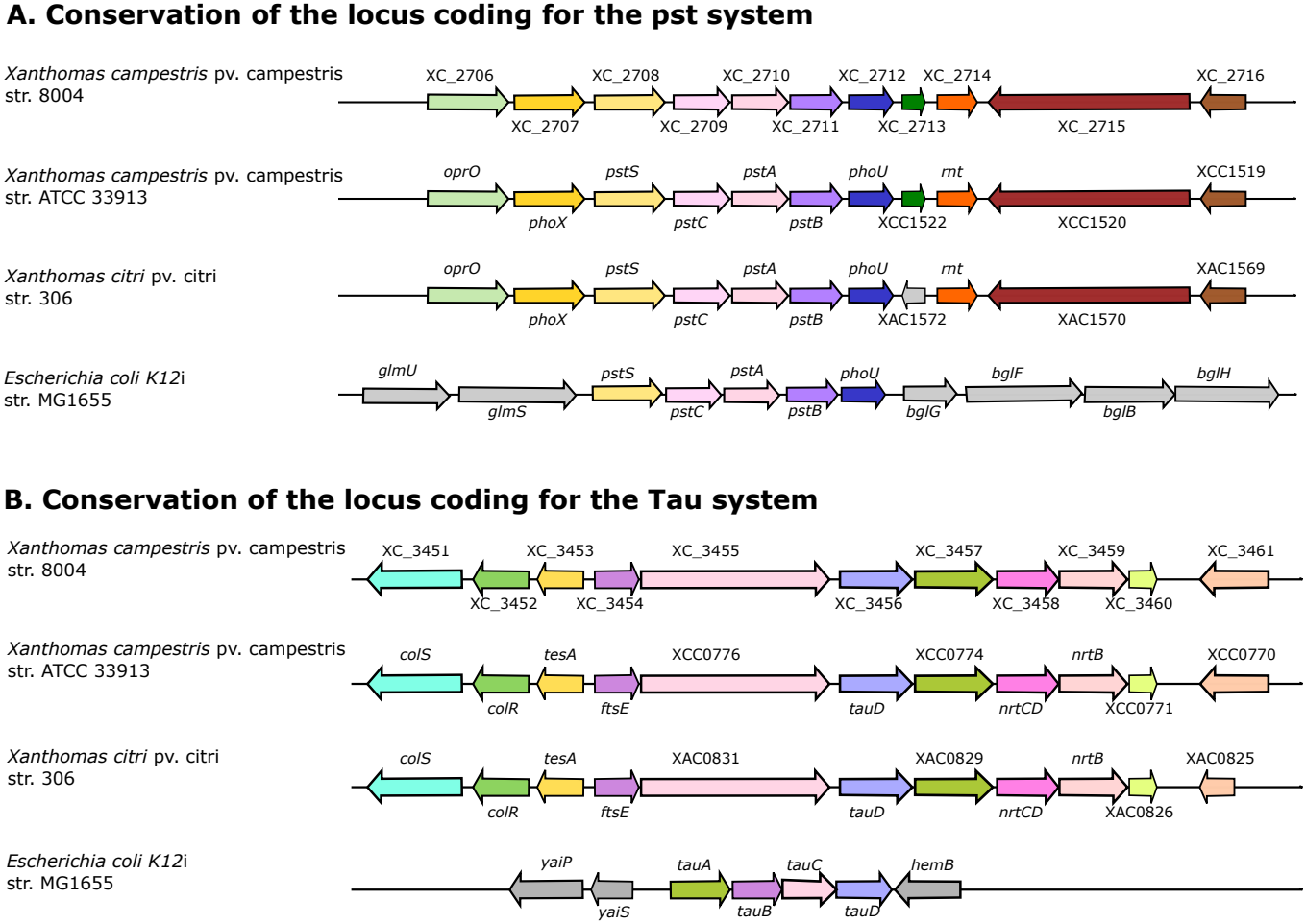

Figure S7. Synteny of genes involved in two transport systems in *Xcc*.
Alignment was performed based on protein Blast using the SyntTax tool (https://archaea.i2bc.paris-saclay.fr/synttax/). (A) Comparison of genetic organization of the locus involved in the pst system between *Xcc* strain 8004, *Xcc* strain ATTC33913, *Xac* strain 306 et *E. coli* K12 strain MG1655 using XC_3456 as reference and "Best match" and a minimal threshold normalized BLAST bit score set at 30% as parameters. (B) Comparison of genetic organization of the locus involved in Tau system between *Xcc* strain 8004, *Xcc* strain ATTC33913, *Xac* strain 306 et *E. coli* K12 strain MG1655 using XC_2711 as reference and "Best match" and a minimal threshold normalized BLAST bit score set at 30% as parameters.

Supplemental Material and Methods

Xanthomonas transcriptome inside cauliflower hydathodes reveals bacterial virulence strategies and physiological adaptation at early infection stages

Julien S. Luneau[1,*], Aude Cerutti[1,*], Brice Roux[1,2], Sébastien Carrère[1], Marie-Françoise Jardinaud[1], Antoine Gaillac[1], Carine Gris[1], Emmanuelle Lauber[1], Richard Berthomé[1], Matthieu Arlat[1], Alice Boulanger[1], Laurent D. Noël[1]

Bacterial pathogenicity assays

Pathogenicity of *Xcc* strains was tested by wound inoculation of the second true leaf of cauliflower plants by wounding the main vein with a needle dipped in an *Xcc* suspension at 10^8 cfu/mL. Symptoms were evaluated according to a disease index scale at 7 and 10 dpi (Figure S5). Experiments were performed on five plants per condition and in three independent biological replicates. Significance of differences observed bacterial pathogenicity assays was assessed using the non-parametric Kruskal-Wallis test with $\alpha = 0.05$.

RNA sequencing procedure

Oriented sequencing was carried out on RNA extracted from *in vitro*-grown *Xcc* by Fasteris SA (Geneva, Switzerland) as described (1). The Small RNA Sequencing Alternative v1.5 Protocol (Illumina) was used for the small RNA fraction, starting with ca. 500 ng RNAs that were treated with tobacco acid pyrophosphatase to remove triphosphate at 5' transcript ends and purified on acrylamide gel before and after the adaptor ligation step. For large RNAs, a fragmentation step by zinc during 8 min was included before the Illumina procedure. The insert size was 20–120 nt for short RNA libraries and 50–120 nt for long RNA libraries. Libraries

were sequenced either in single end (small RNA fraction) or in paired end (Large RNA fraction) on an Illumina HiSeq 2000 platform. Raw sequence data were submitted to the Sequence Read Archive (SRA) database (Accession SRP280320).

For samples prepared from infected tissues, oriented paired-end RNA sequencing was carried out on the GeT-PlaGe platform (Genotoul, Toulouse, France) using an Illumina HiSeq 3000 platform. Oriented RNA libraries were prepared with TrueSep™ Stranded mRNA Sample Prep Kit (Illumina®). Subsequent steps of sequencing were performed according to the manufacturer instructions (RNA fragmentation, ADNc synthesis, 3' adenylation). During the fragmentation step, RNAs were cut in fragments of 120 to 210 nt. Raw sequence data were submitted to the Sequence Read Archive (SRA) database (Accession SRP280329).

Motility assays

Xcc cells grown overnight in MOKA were washed by centrifugation (4000 x g, 5 min) and resuspended in sterile water. 2-µl bacterial suspensions adjusted at 10^8 cfu/mL were spotted on swimming plates (0.03% Bacto peptone, 0.03% yeast extract, 0.3% agar, 2) and incubated 48 h at 28°C. White halos expanding from the colonies indicate the strains' ability to perform flagellar motility.

Protease activity assay on milk plates

10 % skimmed milk stock solution was first autoclave for 10 min and used to pour 0.5 % skimmed milk MOKA plates supplemented with 30µg/mL pimaricin. Each plate contains 15 mL of medium. Extracellular protease activity of *Xcc* strains was tested by spotting 5 µL of an overnight culture adjusted to 4.10^8 cfu/mL. Plates were incubated at 28 °C and imaged 24 hour post inoculation. Diameters of colonies and halos of degradation were measured. Protease

activity was calculated as followed: $PrA = [\pi(r^{halo})^2 - \pi(r^{colo})^2] / [\pi(r^{colo})^2]$ with "r" corresponding to the radius.

Measurement of exopolysaccharide production

Extracellular EPS production was measured as described (3). Briefly, an overnight growth of each strain in MOKA was used to inoculate 20 mL of MOKA supplemented with 50µg/mL of rifampicin at 2.10^7 cfu/mL. After 24 hours of growth 12 mL of culture was centrifuged 15 min at 6500 g. EPS present in supernatant were ethanol precipitated. Then, bacterial and EPS pellets were dried for 8 hours at 65°C before being weighed. EPS production corresponds to the ratio of dry weight EPS on dry weight bacterial cells.

Growth measurements *in vitro*

In vitro growth curves were generated using a FLUOStar Omega apparatus (BMG Labtech, Offenburg, Germany) using 96-well flat-bottom microtiter plates (Greiner) with 200 µL of bacterial suspensions. After an overnight preculture in MOKA rich medium, cells were harvested by centrifugation at 9500 g for 4 minutes, washed and resuspended in MME minimal medium (K_2HPO_4 10.5 g/L, KH_2PO_4 4.5 g/L, $(NH_4)_2SO_4$ 1 g/L $MgSO_4$ 0.12g/L, casamino acids 0.15 g/L) (4). Bacterial suspensions inoculated at an optical density at 600 nm (OD600) of 0.15 were prepared in MME and MOKA media. For each experiment, four replicates coming from two independent precultures were performed. The microplates were shaken continuously at 700 rpm using the linear-shaking mode. Each experiment was repeated three times and a representative experiment was shown.

References

1. Sallet E, Roux B, Sauviac L, Jardinaud MF, Carrere S, Faraut T, et al. Next-Generation Annotation of Prokaryotic Genomes with EuGene-P: Application to *Sinorhizobium meliloti* 2011. DNA Res. 2013;20(4):339-54.

2. Su HZ, Wu L, Qi YH, Liu GF, Lu GT, Tang JL. Characterization of the GntR family regulator HpaR1 of the crucifer black rot pathogen *Xanthomonas campestris* pathovar *campestris*. Sci Rep. 2016;6:19862.

3. Vojnov AA, Zorreguieta A, Dow JM, Daniels MJ, Dankert MA. Evidence for a role for the *gumB* and *gumC* gene products in the formation of xanthan from its pentasaccharide repeating unit by *Xanthomonas campestris*. Microbiology (Reading). 1998;144 (Pt 6):1487-93.

4. Arlat M, Gough CL, Barber CE, Boucher C, Daniels MJ. *Xanthomonas campestris* contains a cluster of *hrp* genes related to the larger *hrp* cluster of *Pseudomonas solanacearum*. Mol Plant Microbe Interact. 1991;4(6):593-601.